Computers and Mathematics with Applications 76 (2018) 340–360

Contents lists available at ScienceDirect

Computers and Mathematics with Applications

journal homepage: www.elsevier.com/locate/camwa

A posteriori error analysis of the fully discretized time-dependent coupled Darcy and Stokes equations

Christine Bernardi [a,b], Ajmia Younes Orfi [c,*]

[a] CNRS, UMR 7598, Laboratoire Jacques-Louis Lions, F-75005, Paris, France
[b] Sorbonne Universits, UPMC Univ Paris 06, UMR 7598, LJLI, F-75005, Paris, France
[c] University of Tunis El Manar, Faculty of Sciences, 2060 Tunis, Tunisia

ARTICLE INFO

Article history:
Received 28 July 2017
Received in revised form 9 April 2018
Accepted 15 April 2018
Available online 18 May 2018

Keywords:
A posteriori error analysis
Darcy equations
Stokes equations
Backward Euler scheme
Finite elements

ABSTRACT

We present an a posteriori error analysis of the fully discretized time-dependent Darcy and Stokes equations, that models laminar fluid flow over a porous medium in two- or three-dimensional connected open domains which are coupled via appropriate matching conditions on the interface. The problem is discretized by the backward Euler scheme in time and finite elements in space.

© 2018 Elsevier Ltd. All rights reserved.

1. Introduction

The coupled models find numerous practical applications, for example the flow of blood in arteries, diffusion and dispersion of pollutants in water, the flow with heat transfer in porous media, etc. These coupled problems involve several partial differential equations such as the Navier–Stokes equations, the Stokes equations, the Darcy's law in porous region and the free surface Navier–Stokes equations, [1–4]. The flow inside a deformable tube can be modeled using the linear elasticity equations coupled with the Navier–Stokes equations.

In this paper, we focus on a model for a liquid such as water flowing on a homogeneous porous ground, where the instationary Darcy and Stokes equations are coupled via appropriate matching conditions on the interface. This kind of problem is studied in [5] for the stationary case.

One important issue in the coupled Darcy–Stokes flow is the treatment of the interface condition, where the Stokes fluid meets the porous medium.

[3,6–14] considered a formulation based on the Beaver–Joseph–Saffman interface conditions, which was experimentally derived by Beavers and Joseph in [15]. For these Darcy–Stokes equations, the following interface conditions have been extensively studied and used in literature see [3,11] and [16, Sec. 4.5]

$$\boldsymbol{u}|_{\Omega_P}\cdot\boldsymbol{n}=\boldsymbol{u}|_{\Omega_F}\cdot\boldsymbol{n}\quad\text{and}\quad -p|_{\Omega_P}\boldsymbol{n}=\nu\partial_n\boldsymbol{u}|_{\Omega_F}-p|_{\Omega_F}\boldsymbol{n}\quad\text{on }\Gamma\times]0,T[,\tag{1}$$

the first and the second interface conditions ensure the mass conservation and the continuity of forces, respectively, across the interface Γ. However, in [8] the interface conditions refer to mass conservation, balance of normal forces in addition

* Corresponding author.
E-mail addresses: bernardi@ann.jussieu.fr (C. Bernardi), ayounesorfi@yahoo.com (A.Y. Orfi).

https://doi.org/10.1016/j.camwa.2018.04.021
0898-1221/© 2018 Elsevier Ltd. All rights reserved.

to the Beavers–Joseph–Saffman law, which yields the introduction of the trace of the porous media pressure as a suitable Lagrange multiplier.

Various numerical methods, such as finite element methods, mixed methods, discontinuous Galerkin methods and combinations of these methods, have been studied in the literature. For instance, finite element methods were studied in [3] and finite element methods coupled with mixed methods have been analyzed in [11]. Primal discontinuous Galerkin methods using broken Sobolev spaces are analyzed in [12], and they are coupled with mixed methods in [13].

The stability of the numerical methods for the evolutionary Stokes–Darcy problem was analyzed in different previous works see [17–19]. For example, [19] proposed an approach consisting of four methods that uncouple each time step into separate Stokes flow problem and Darcy flow problem, one is a parallel uncoupling method, while the three others uncouple sequentially. In [17] a second order and unconditionally stable method for the unsteady Stokes–Darcy problem is proposed. This method uncouples the surface from the groundwater flow by using the implicit–explicit combination of the Crank–Nicolson and Leapfrog methods for the discretization in time.

The basic discretization of this problem relies on the backward Euler scheme with respect to the time variable and on finite elements with respect to the space variables. The space discretization that we propose relies on the mortar element method, a domain decomposition technique introduced in [20] and [21]. We use a subdomain for the fluid and another one for the porous medium. On each subdomain, we consider a finite element discretization, relying on standard finite elements both for the Stokes problem and the Darcy equations. For the Stokes problem we use the Bernardi–Raugel finite element introduced in [22] and analyzed in [23] and for the Darcy problem we use the Raviart–Thomas finite element, see [24]. Besides, in [8] the same finite elements are employed for the Stokes and the Darcy domains, whereas the Lagrange multiplier on the interface is approximated by continuous piecewise linear elements.

Other choices of finite elements are possible. Indeed, the Raviart–Thomas element is the simplest div-conforming element and the Bernardi–Raugel element is the less expensive H^1-conforming finite element for the Stokes problem.

The a priori analysis of this problem has been recently published, see [25]. The aim of the present paper is to extend the investigation to the a posteriori analysis.

Several works have been done concerning the a posteriori analysis of parabolic type problems. Part of it (*cf*. [26–28]) deals only with the space discretization and provides appropriate error indicators for it. Another idea see [29–31], consists in establishing a full time and space variational formulation of the continuous problem and using a discontinuous Galerkin method for the discretization with respect to all variables. In this work, we follow a different approach that uncouples as much as possible the time and space errors, according to an idea presented in [32]. We introduce two different types of error indicators, one for the time discretization and other for the space discretization, and we prove upper and lower bounds for the error.

An outline of the paper is as follows:

• Section 2 is devoted to the description of the continuous, the time semi-discrete and the fully discrete problems. We recall their main properties and some standard a priori estimates.
• In Section 3, we perform the a posteriori analysis of the time discretization.
• In Section 4, three families of error indicators, related to the error on Ω_P, Ω_F and Γ, respectively, are proposed and the a posteriori analysis of the discrete problem is achieved.
• The adaptivity strategy is presented in Section 5.

2. The continuous, semi-discrete and discrete problems

The mortar element method has been used for handling curved boundaries. In order to avoid the techniques required for the treatment of the curved boundaries, we assume that the domain Ω is a polygonal in dimension $(d = 2)$ or a polyhedral in dimension $(d = 3)$ divided into two connected open sets Ω_P and Ω_F with Lipschitz-continuous boundaries, where the indices P and F stand for porous and fluid, respectively. Let $T > 0$ be a finite time. The fluid that we consider is viscous and incompressible and is governed by the Stokes equations:

$$\begin{cases} \partial_t \boldsymbol{u} - \nu \Delta \boldsymbol{u} + \mathbf{grad} p = \boldsymbol{f} & \text{in} \quad \Omega_F \times]0, T[, \\ \mathrm{div} \boldsymbol{u} = 0 & \text{in} \quad \Omega_F \times]0, T[, \\ \boldsymbol{u}(\boldsymbol{x}, 0) = \boldsymbol{u}^0(\boldsymbol{x}) & \text{in} \quad \Omega_F \quad \text{at} \quad t = 0. \end{cases} \tag{2}$$

The porous medium is assumed to be rigid and saturated with the fluid, and governed by the Darcy equations:

$$\begin{cases} \partial_t \boldsymbol{u} + \alpha \boldsymbol{u} + \mathbf{grad} p = \boldsymbol{f} & \text{in} \quad \Omega_P \times]0, T[, \\ \mathrm{div} \boldsymbol{u} = 0 & \text{in} \quad \Omega_P \times]0, T[, \\ \boldsymbol{u}(\boldsymbol{x}, 0) = \boldsymbol{u}^0(\boldsymbol{x}) & \text{in} \quad \Omega_P \quad \text{at} \quad t = 0. \end{cases} \tag{3}$$

In problems (2) and (3) the unknowns are the velocity $\boldsymbol{u}$ and the pressure p of the fluid; the data are the distribution $\boldsymbol{f}$ which represents the external force and the initial velocity $\boldsymbol{u}^0$, while the parameters ν and α are positive constants, representing the viscosity of the fluid and the ratio of this viscosity to the permeability of the medium, respectively. We assume that α is a constant on Ω_P, which implies that the porous medium is homogeneous, see [33] and [34]. Concerning

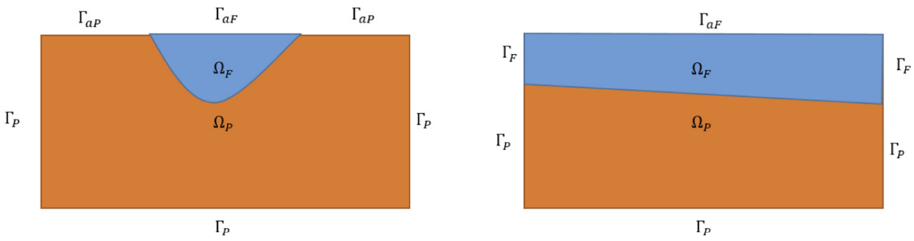

Fig. 1. Two examples of two-dimensional domains Ω.

the boundary conditions, as illustrated in Fig. 1 ($d = 2$), we denote by Γ_a the upper edge ($d = 2$) or face ($d = 3$) of Ω, where the index a means in contact with the atmosphere. Let $\Gamma_{aP} = \Gamma_a \cap \partial\Omega_P$, and $\Gamma_{aF} = \Gamma_a \cap \partial\Omega_F$. We set $\Gamma_P = (\partial\Omega \cap \partial\Omega_P) \setminus \Gamma_{aP}$, and $\Gamma_F = (\partial\Omega \cap \partial\Omega_F) \setminus \Gamma_{aF}$. Let $\boldsymbol{n}$ the unit outward normal vector to Ω and also to Ω_P on $\partial\Omega_P$. We provide the previous partial differential equations (2) and (3) with the conditions

$$\boldsymbol{u} \cdot \boldsymbol{n} = k \quad \text{on } \Gamma_P \times]0, T[\quad \text{and} \quad p = p_a \quad \text{on } \Gamma_{aP} \times]0, T[, \tag{4}$$

$$\boldsymbol{u} = \boldsymbol{g} \quad \text{on } \Gamma_F \times]0, T[\quad \text{and} \quad \nu\partial_n \boldsymbol{u} - p\boldsymbol{n} = \boldsymbol{t}_a \quad \text{on } \Gamma_{aF} \times]0, T[. \tag{5}$$

On $\partial\Omega \setminus \Gamma_a$ these conditions are Dirichlet type, on Γ_{aP} the pressure is equal to the atmospheric pressure p_a, on Γ_{aF} the variations of the free surface at the top of the flow are neglected in the model, thus $\boldsymbol{t}_a$ depends on the atmospheric pressure and the wind on the river. However, see [35, Sec. 1.4], when $\Gamma_{aP} = \Gamma_{aF} = \phi$, the flux condition $\int_{\Gamma_F} (\boldsymbol{g} \cdot \boldsymbol{n})(\tau)\, d\tau + \int_{\Gamma_P} k(\tau)\, d\tau = 0$, is necessary both mathematically and due to the physics of the problem.

Let Γ denotes the interface $\partial\Omega_P \cap \partial\Omega_F$. On Γ we consider the matching conditions (1).

2.1. Variational formulation

Let $H(\text{div}, \Omega)$ denotes the space of functions v in $L^2(\Omega)^d$ such that $\text{div}(v)$ belongs to $L^2(\Omega)$. $H(\text{div}, \Omega)$ is Hilbert space for the scalar product associated with the following norm

$$\|v\|_{H(\text{div};\,\Omega)} = \left(\|v\|^2_{L^2(\Omega)^d} + \|\text{div}(v)\|^2_{L^2(\Omega)}\right)^{\frac{1}{2}}.$$

In all that follows, for any t, $0 < t \le T$, and any separable Banach space X provided with the norm $\|\cdot\|_X$, we denote by $L^2(0, t; X)$ the space of measurable functions v from $(0, t)$ in X such that

$$\|v\|_{L^2(0,t;X)} = \left(\int_0^t \|v(\cdot, t)\|_X^2\, dt\right)^{\frac{1}{2}} < +\infty.$$

For any positive integer m, we introduce the space $H^m(0, t; X)$ of functions in $L^2(0, t; X)$ such that all their time derivatives of order $\le m$ belong to $L^2(0, t; X)$ and equipped with the norm

$$\|u\|_{H^1(0,t;X)} = \left(\int_0^t \|u(\cdot, t)\|_X^2\, dt + \int_0^t \|\partial_t u(\cdot, t)\|_X^2\, dt\right)^{\frac{1}{2}}.$$

We also use the space $C^0(0, t; X)$ of continuous functions v from $[0, t]$ in X. Let $(\cdot, \cdot)$ stands for the scalar product on $L^2(\Omega)$ or $L^2(\Omega)^d$.

Finally, we introduce the variational spaces

$$X(\Omega) = \left\{\boldsymbol{v} \in H(\text{div};\, \Omega);\ \boldsymbol{v}|_{\Omega_F} \in H^1(\Omega_F)^d\right\},$$

$$X_0(\Omega) = \{\boldsymbol{v} \in X(\Omega);\ \boldsymbol{v} \cdot \boldsymbol{n} = 0 \text{ on } \Gamma_P \text{ and } \boldsymbol{v} = 0 \text{ on } \Gamma_F\}.$$

Both of them are Hilbert spaces equipped with the norm

$$\|\boldsymbol{v}\|_{X(\Omega)} = (\|\boldsymbol{v}\|^2_{H(\text{div};\Omega_P)} + \|\boldsymbol{v}\|^2_{H^1(\Omega_F)^d})^{\frac{1}{2}}.$$

For convenience, throughout this paper, we will use the notation $x \lesssim y$ to denote that $x \le cy$, where c is a positive constant.

Remark 1. We know that the normal trace operator $\boldsymbol{v} \mapsto \boldsymbol{v} \cdot \boldsymbol{n}$ is defined and continuous from $H(\text{div};\, \Omega)$ into $H^{-\frac{1}{2}}(\partial\Omega)$ see [36, Chap. I , Thm. 2.4]. Moreover, for any part Γ^* of $\partial\Omega$ with positive measure, the normal trace on Γ^* of a function $\boldsymbol{v}$

in $H(\mathrm{div};\Omega)$ makes sense in $H_{00}^{\frac{1}{2}}(\Gamma^*)'$, note in addition that $H^{-\frac{1}{2}}(\Gamma^*)$ is imbedded in $H_{00}^{\frac{1}{2}}(\Gamma^*)'$. We refer to [37, Chap. I, Sec. 11], for the definition of $H_{00}^{\frac{1}{2}}(\Gamma^*)$ as the space of functions in $H^{\frac{1}{2}}(\Gamma^*)$ such that their extension by zero belongs to $H^{\frac{1}{2}}(\partial\Omega)$.

Assume that the data

$$\begin{aligned} &\boldsymbol{f} \in L^2(0,T;X_0(\Omega)'),\ p_a \in L^2(0,T;H_{00}^{\frac{1}{2}}(\Gamma_{aP})), k \in L^2(0,T;H^{-\frac{1}{2}}(\Gamma_P)),\\ &\boldsymbol{t}_a \in L^2(0,T;H^{-\frac{1}{2}}(\Gamma_{aF})^d), \boldsymbol{g} \in L^2(0,T;H^{\frac{1}{2}}(\Gamma_F)^d) \text{ and } \boldsymbol{u}^0 \in X(\Omega). \end{aligned} \tag{6}$$

It can be checked that problem (2) to (1) admits the variational formulation:

Find $\boldsymbol{u} \in L^2(0,T;X(\Omega)) \cap C^0(0,T;L^2(\Omega)^d)$ and $p \in L^2(0,T;L^2(\Omega))$ such that

$$\boldsymbol{u}(\cdot,0) = \boldsymbol{u}^0 \quad \text{in } \Omega, \tag{7}$$

such that, for a.e. $t,\ 0 \le t \le T$

$$\begin{aligned} &\boldsymbol{u}(\cdot,t)\cdot\boldsymbol{n} = k(\cdot,t) && \text{on } \Gamma_P,\\ &\boldsymbol{u}(\cdot,t) = \boldsymbol{g}(\cdot,t) && \text{on } \Gamma_F, \end{aligned} \tag{8}$$

and such that, for a.e. $t,\ 0 \le t \le T$,

$$\begin{aligned} &\forall \boldsymbol{v} \in X_0(\Omega), \quad (\partial_t\boldsymbol{u},\boldsymbol{v}) + a(\boldsymbol{u},\boldsymbol{v}) + b(\boldsymbol{v},p) = \mathcal{L}(\cdot,t)(\boldsymbol{v}),\\ &\forall q \in L^2(\Omega), \quad b(\boldsymbol{u},q) = 0, \end{aligned} \tag{9}$$

where $a(\boldsymbol{u},\boldsymbol{v}) = a_{\Omega_F}(\boldsymbol{u},\boldsymbol{v}) + a_{\Omega_P}(\boldsymbol{u},\boldsymbol{v})$,

$$a_{\Omega_F}(\boldsymbol{u},\boldsymbol{v}) = \nu\int_{\Omega_F}\nabla\boldsymbol{u}(\boldsymbol{x},t):\nabla\boldsymbol{v}(\boldsymbol{x})\,d\boldsymbol{x}, \quad a_{\Omega_P}(\boldsymbol{u},\boldsymbol{v}) = \alpha\int_{\Omega_P}\boldsymbol{u}(\boldsymbol{x},t)\cdot\boldsymbol{v}(\boldsymbol{x})\,d\boldsymbol{x},$$

$$b(\boldsymbol{v},q) = -\int_\Omega \mathrm{div}\boldsymbol{v}(\boldsymbol{x})\,q(\boldsymbol{x})\,d\boldsymbol{x},$$

$$\begin{aligned} \text{and} \qquad \mathcal{L}(\cdot,t)(\boldsymbol{v}) = &\int_\Omega \boldsymbol{f}(\boldsymbol{x},t)\cdot\boldsymbol{v}(\boldsymbol{x})\,d\boldsymbol{x} - \int_{\Gamma_{aP}}(\boldsymbol{v}\cdot\boldsymbol{n})(\tau)\,p_a(\boldsymbol{x},t)(\tau)\,d\tau\\ &+ \int_{\Gamma_{aF}}\boldsymbol{v}(\tau)\cdot\boldsymbol{t}_a(\boldsymbol{x},t)(\tau)\,d\tau. \end{aligned} \tag{10}$$

It is readily checked that $a(\cdot,\cdot)$ is continuous on $X(\Omega)\times X(\Omega)$, while the bilinear form $b(\cdot,\cdot)$ is continuous on $X(\Omega)\times L^2(\Omega)$; its kernel

$$V(\Omega) = \left\{\boldsymbol{v} \in X_0(\Omega);\ \forall q \in L^2(\Omega),\ b(\boldsymbol{v},q) = 0\right\},$$

coincides with the space of functions in $X_0(\Omega)$ which are divergence-free on Ω.

Assumption 1. We assume that:
(i) either Γ_F has a positive measure in $\partial\Omega_F$,
(ii) or the normal vector $\boldsymbol{n}(\boldsymbol{x})$ runs through a basis of $\mathbb{R}^d$ when $\boldsymbol{x}$ runs through Γ.

Recalling the main results concerning this problem, see [25] and also ([5, Lems 2.5 and 2.6]) which are proven:
(i) If Assumption 1 is satisfied, then the following ellipticity property holds for $\alpha_* = \min(\nu,\alpha)$

$$\forall \boldsymbol{v} \in V(\Omega), \quad \alpha_*\,\|\boldsymbol{v}\|_{X(\Omega)}^2 \lesssim a(\boldsymbol{v},\boldsymbol{v}), \tag{11}$$

where, see the proof in [5, Lem 2.5]

$$\forall \boldsymbol{v} \in V(\Omega), \quad \|\boldsymbol{v}\|_{X(\Omega)} \lesssim \left(\|\boldsymbol{v}\|_{L^2(\Omega_P)^d}^2 + |\boldsymbol{v}|_{H^1(\Omega_F)^d}^2\right)^{\frac{1}{2}}. \tag{12}$$

(ii) There exists a constant $\beta > 0$ such that

$$\forall q \in L^2(\Omega), \quad \sup_{\boldsymbol{v}\in X_0(\Omega)}\frac{b(\boldsymbol{v},q)}{\|\boldsymbol{v}\|_{X(\Omega)}} \ge \beta\,\|q\|_{L^2(\Omega)}. \tag{13}$$

To study this problem, we will take $\boldsymbol{t}_a = k = \boldsymbol{g} = 0$ which is not fully unlikely from a physical point of view, and assume the following:

$$\boldsymbol{f} \in L^2(0,T;L^2(\Omega)^d),\ p_a \in L^2(0,T;H_{00}^{\frac{1}{2}}(\Gamma_{aP})),\ \text{ and } \boldsymbol{u}^0 \in X_0(\Omega). \tag{14}$$

A new variational formulation equivalent to problem (7)–(8)–(9) was found in [25] when $\boldsymbol{t}_a = 0$. For this, since $p_a \in L^2(0,T;H_{00}^{\frac{1}{2}}(\Gamma_{aP}))$, there exists a lifting $\tilde{p}_a \in L^2(0,T;H^1(\Omega))$ such that $\tilde{p}_a = 0$ on $\partial\Omega \setminus \Gamma_{aP}$ and

$$\left\|\tilde{p}_a\right\|_{L^2(0,T;H^1(\Omega))} \lesssim \|p_a\|_{L^2(0,T;H_{00}^{\frac{1}{2}}(\Gamma_{aP}))}. \tag{15}$$

We set: $p_* = p - \tilde{p}_a$, where $p_*|_{\Gamma_{aP}} = 0$. We observe that problem (7)–(8)–(9) is equivalent to the following:

Find $\boldsymbol{u} \in L^2(0,T;X_0(\Omega)) \cap C^0(0,T;L^2(\Omega)^d)$ and $p_* \in L^2(0,T;L^2(\Omega))$ such that,

$$\boldsymbol{u}(\cdot,0) = \boldsymbol{u}^0 \quad \text{in } \Omega, \tag{16}$$

and for a.e. t, $0 \le t \le T$,

$$\begin{aligned} &\forall \boldsymbol{v} \in X_0(\Omega), \qquad (\partial_t \boldsymbol{u}, \boldsymbol{v}) + a(\boldsymbol{u}, \boldsymbol{v}) + b(\boldsymbol{v}, p_*) = L(\cdot,t)(\boldsymbol{v}),\\ &\forall q \in L^2(\Omega), \qquad b(\boldsymbol{u}, q) = 0, \end{aligned} \tag{17}$$

where

$$L(\cdot,t)(\boldsymbol{v}) = \int_\Omega \boldsymbol{f}(\boldsymbol{x},t)\cdot\boldsymbol{v}(\boldsymbol{x})\,d\boldsymbol{x} - \int_\Omega \nabla\tilde{p}_a(\boldsymbol{x},t)\cdot\boldsymbol{v}(\boldsymbol{x})\,d\boldsymbol{x}. \tag{18}$$

Furthermore, the following existence and stability results are derived from [25, Sect. 2.2, Thm. 3].

Theorem 1. *If Assumption 1 holds, in the case $\boldsymbol{t}_a = k = \boldsymbol{g} = 0$ and for any data $(\boldsymbol{f}, p_a, \boldsymbol{u}^0)$ satisfying (14), problem (7)– (8)–(9) has a unique solution*

$$\boldsymbol{u} \in L^2(0,T;X(\Omega)) \cap C^0(0,T;L^2(\Omega)^d) \text{ and } p \in L^2(0,T;L^2(\Omega))$$

such that

$$\begin{aligned} &\|\boldsymbol{u}\|_{H^1(0,T;L^2(\Omega)^d)} + \|\boldsymbol{u}\|_{L^2(0,T;X(\Omega))} + \|p\|_{L^2(0,T;L^2(\Omega))}\\ &\lesssim \|\boldsymbol{f}\|_{L^2(0,t;L^2(\Omega)^d)} + \|p_a\|_{L^2(0,t;H_{00}^{\frac{1}{2}}(\Gamma_{aP}))} + \|\boldsymbol{u}(\cdot,0)\|_{X(\Omega)}. \end{aligned} \tag{19}$$

2.2. The time semi-discrete problem

In order to describe the time discretization of problem (2) to (1) with an adaptive choice of local time steps, we introduce a partition of the interval $[0,T]$ into subintervals $[t_{n-1}, t_n]$, $1 \le n \le N$, such that $0 = t_0 < t_1 < \cdots < t_N = T$. We denote by τ_n the length $t_n - t_{n-1}$, by τ the N-tuple $(\tau_1, \tau_2, \cdots, \tau_N)$, and by $|\tau|$ the maximum of the τ_n, $1 \le n \le N$. For any data $(\boldsymbol{f}, p_a, k, \boldsymbol{t}_a, \boldsymbol{g}, \boldsymbol{u}_0)$ satisfying

$$\begin{aligned} &\boldsymbol{f} \in \mathcal{C}^0(0,T;X_0(\Omega)'),\ p_a \in \mathcal{C}^0(0,T;H_{00}^{\frac{1}{2}}(\Gamma_{aP})), k \in \mathcal{C}^0(0,T;H^{-\frac{1}{2}}(\Gamma_P)),\\ &\boldsymbol{t}_a \in \mathcal{C}^0(0,T;H^{-\frac{1}{2}}(\Gamma_{aF})^d), \boldsymbol{g} \in \mathcal{C}^0(0,T;H^{\frac{1}{2}}(\Gamma_F)) \text{ and } \boldsymbol{u}^0 \in X(\Omega). \end{aligned} \tag{20}$$

The semi-discrete problem constructed from the backward Euler scheme applied to the variational formulation (7)–(8)–(9) is:

Find $(\boldsymbol{u}^n)_{0\le n\le N}$, in $(X(\Omega))^{N+1}$ and $(p^n)_{1\le n\le N}$ in $\left(L^2(\Omega)\right)^N$ such that

$$\boldsymbol{u}^0 = \boldsymbol{u}(\cdot,0) \quad \text{in} \quad \Omega, \tag{21}$$

such that, for all n, $1 \le n \le N$,

$$\boldsymbol{u}^n\cdot\boldsymbol{n} = k^n \quad \text{on} \quad \Gamma_P, \quad \boldsymbol{u}^n = \boldsymbol{g}^n \quad \text{on} \quad \Gamma_F, \tag{22}$$

and, for all n, $1 \le n \le N$,

$$\begin{aligned} &\forall \boldsymbol{v} \in X_0(\Omega),\ (\boldsymbol{u}^n, \boldsymbol{v}) + \tau_n a(\boldsymbol{u}^n, \boldsymbol{v}) + \tau_n b(\boldsymbol{v}, p^n) = (\boldsymbol{u}^{n-1}, \boldsymbol{v}) + \tau_n \mathcal{L}^n(\boldsymbol{v}),\\ &\forall q \in L^2(\Omega),\ b(\boldsymbol{u}^n, q) = 0, \end{aligned} \tag{23}$$

where $k^n = k(\cdot,t_n)$, $\boldsymbol{g}^n = \boldsymbol{g}(\cdot,t_n)$, $\boldsymbol{f}^n = \boldsymbol{f}(\cdot,t_n)$, $\boldsymbol{t}_a^n = \boldsymbol{t}_a(\cdot,t_n)$, $p_a^n = p_a(\cdot,t_n)$ and $\mathcal{L}^n(\boldsymbol{v}) = \mathcal{L}(\cdot,t_n)(\boldsymbol{v})$ ($\mathcal{L}$ is defined in (10)).

When $\boldsymbol{t}_a = 0$, a new variational formulation equivalent to problem (21)–(22)–(23) was found in [25, Sect. 3.1]. Here, similar than previous, we assume that $\boldsymbol{t}_a = k = \boldsymbol{g} = 0$ and we will find a new variational formulation which is equivalent to problem (21)–(22)–(23). For this we use $\tilde{p}_a^n = \tilde{p}_a(\cdot,t_n) \in H^1(\Omega)$ defined in (15) such that

$$\left\|\tilde{p}_a^n\right\|_{H^1(\Omega)} \lesssim \left\|p_a^n\right\|_{H_{00}^{\frac{1}{2}}(\Gamma_{aP})}. \tag{24}$$

We set: $p_*^n = p^n - \tilde{p}_a^n$. We observe that problem (21)–(22)–(23) is equivalent to the following:

Find $\big((\boldsymbol{u}^n)_{0\le n\le N}, (p_*^n)_{1\le n\le N}\big) \in (X_0(\Omega))^{N+1} \times (L^2(\Omega))^N$ such that

$$\boldsymbol{u}^0 = \boldsymbol{u}(\cdot, 0) \quad \text{in} \quad \Omega, \tag{25}$$

$$\begin{aligned} &\forall \boldsymbol{v} \in X_0(\Omega), \qquad (\boldsymbol{u}^n - \boldsymbol{u}^{n-1}, \boldsymbol{v}) + \tau_n a(\boldsymbol{u}^n, \boldsymbol{v}) + \tau_n b(\boldsymbol{v}, p_*^n) = \tau_n L^n(\boldsymbol{v}), \\ &\forall q \in L^2(\Omega), \qquad b(\boldsymbol{u}^n, q) = 0, \end{aligned} \tag{26}$$

where, $L^n(\boldsymbol{v}) = L(\cdot, t_n)(\boldsymbol{v}) = (\boldsymbol{f}^n, \boldsymbol{v}) - (\nabla \tilde{p}_a^n, \boldsymbol{v})$ (L is defined in (18)).

To conclude, we recall the following regularity property of the solution of problem (21)–(22)–(23) see [25, Sect. 3.1, Props 1, 2 and 3].

Proposition 1. *In the case $\mathbf{t}_a = k = \boldsymbol{g} = 0$ and for any data $(\boldsymbol{f}, p_a, \boldsymbol{u}^0)$ satisfying (20), problem (21)–(22)–(23) has a unique solution $(\boldsymbol{u}^n)_{0\le n\le N}$ in $(X(\Omega))^{N+1}$ and $(p^n)_{1\le n\le N}$ in $\big(L^2(\Omega)\big)^N$ such that*

$$\Big(\|\boldsymbol{u}^n\|^2_{L^2(\Omega)^d} + \alpha_* \sum_{m=1}^n \tau_m \|\boldsymbol{u}^m\|^2_{X(\Omega)}\Big)^{\frac12} \lesssim \|\boldsymbol{u}^0\|_{X(\Omega)} + \frac{1}{\sqrt{\alpha_*}}\Big(\sum_{m=1}^n \tau_m\big(\|\boldsymbol{f}^m\|^2_{L^2(\Omega)^d} + \|p_a^m\|^2_{H^{\frac12}(\Gamma_{aP})}\big)\Big)^{\frac12},$$

and

$$\Big(\sum_{m=1}^n \tau_m \Big\|\frac{\boldsymbol{u}^m - \boldsymbol{u}^{m-1}}{\tau_m}\Big\|^2_{L^2(\Omega)^d} + \tau_m \|p^m\|^2_{L^2(\Omega)}\Big)^{\frac12} \lesssim \frac{1}{\sqrt{\alpha_*}}\|\boldsymbol{u}^0\|_{X(\Omega)} + \Big(1 + \frac{1}{(\alpha_*)^2}\Big)^{\frac12}\Big(\sum_{m=1}^n \tau_m\big(\|\boldsymbol{f}^m\|^2_{X_0(\Omega)'} + \|p_a^m\|^2_{H^{\frac12}(\Gamma_{aP})}\big)\Big)^{\frac12}.$$

2.3. The time and space discrete problem

We now describe the space discretization of problem (21)–(22)–(23). For each n, $0 \le n \le N$, we introduce regular families $(\mathcal{T}_{nh}^P)_{h_P}$ and $(\mathcal{T}_{nh}^F)_{h_F}$ of triangulations of Ω_P and Ω_F, respectively, by closed triangles ($d = 2$) or tetrahedra ($d = 3$), also we denote by $\mathcal{T}_{nh}$, the union of $\mathcal{T}_{nh}^P$ and $\mathcal{T}_{nh}^F$. As usual, h_{nP} stands for the maximum of the diameters of the elements of $\mathcal{T}_{nh}^P$, h_{nF} for the maximum of the diameters of the elements of $\mathcal{T}_{nh}^F$ and $h_n = \max\{h_{nP}, h_{nF}\}$. We assume as in [5] that:

- For each h_{nP}, $\overline{\Omega}_P$ is the union of all elements of $\mathcal{T}_{nh}^P$ and, for each h_{nF}, $\overline{\Omega}_F$ is the union of all elements of $\mathcal{T}_{nh}^F$.
- The intersection of two different elements of $\mathcal{T}_{nh}^P$, if not empty, is a vertex or a whole edge or a whole face of both of them, and the same property holds for the intersection of two different elements of $\mathcal{T}_{nh}^F$.
- The ratio of the diameter h_K of any element K of $\mathcal{T}_{nh}^P$ or $\mathcal{T}_{nh}^F$ to the diameter of its inscribed circle or sphere is smaller than a constant σ independent of h_P, h_F, n, and K.

Assumption 2. The intersection of each element K of $\mathcal{T}_{nh}^P$ with either $\overline{\Gamma}_{aP}$ or $\overline{\Gamma}_P$ or $\overline{\Gamma}$, if not empty, is a vertex or a whole edge or a whole face of K. The intersection of each element K of $\mathcal{T}_{nh}^F$ with either $\overline{\Gamma}_{aF}$ or $\overline{\Gamma}_F$ or $\overline{\Gamma}$, if not empty, is a vertex or a whole edge or a whole face of K.

It must be noted that, up to now, no assumption is made on the intersection of the elements of $\mathcal{T}_{nh}^P$ and $\mathcal{T}_{nh}^F$. So the $K \cap \Gamma$, $K \in \mathcal{T}_{nh}^P$, and the $K \cap \Gamma$, $K \in \mathcal{T}_{nh}^F$, form two independent triangulations of Γ, that we denote by $\mathcal{E}_{nh}^{P,\Gamma}$ and $\mathcal{E}_{nh}^{F,\Gamma}$, respectively. However, we are led to make another assumption.

Assumption 3. For element K of $\mathcal{T}_{nh}^F$, the number of elements K' of $\mathcal{T}_{nh}^P$ such that $\partial K \cap \partial K'$ has a positive (d-1)-measure is bounded independently of K, h_P and h_F.

Remark 2. Let K be any element of $\mathcal{T}_{nh}^F$ which has an edge ($d = 2$) or a face ($d = 3$) e contained in Γ. Assumption 3 yields that e is contained in the union of edges or faces e_i, $1 \le i \le I$, of elements K_i of $\mathcal{T}_{nh}^P$ where I is bounded independently of K and h.

From now on, $P_\ell(K)$ denote the space of restriction to K of polynomials on $\mathbb{R}^d$, with degree $\le \ell$.

We now define the local discrete spaces. On Ω_P, we introduce the following discrete space which is constructed from the Raviart–Thomas element $RT_0(K)$ see [24]:

$$X_{nh}^P = \left\{ \boldsymbol{v}_h \in H(\mathrm{div}; \Omega_P);\ \forall K \in \mathcal{T}_{nh}^P,\ \boldsymbol{v}_h\big|_K \in RT_0(K) \right\},$$

where

$$RT_0(K) = P_0(K)^d + \boldsymbol{x}\, P_0(K).$$

Indeed, it is the simplest and less expensive element which is conforming in the domain of divergence operator, so that we use it on Ω_P.

We define the space

$$X_{0nh}^P = \left\{ \boldsymbol{v}_h \in X_{nh}^P;\ \boldsymbol{v}_h \cdot \boldsymbol{n} = 0 \text{ on } \Gamma_P \right\}.$$

We introduce the Raviart–Thomas operator Π_{nh}^{RT}, see [24, Sec. 3] and also [38, Sec. 1.3], for its three-dimensional analogue: For any smooth enough function $\boldsymbol{v}$ on Ω_P, $\Pi_{nh}^{RT}\boldsymbol{v}$ belongs to X_{nh}^P and satisfies on all edges ($d = 2$) or faces ($d = 3$) e of elements of $\mathcal{T}_{nh}^P$

$$\int_e (\Pi_{nh}^{RT}\boldsymbol{v} \cdot \boldsymbol{n})(\tau)\, d\tau = \int_e (\boldsymbol{v} \cdot \boldsymbol{n})(\tau)\, d\tau.$$

The fact that these equations define the operator Π_{nh}^{RT} in a unique way and its main properties are proved in [24, Thm. 3], in the two-dimensional case. This operator preserves the nullity of the normal trace on Γ_P (this requires Assumption 2).

On Ω_F, we introduce the following discrete space which is constructed from the Bernardi–Raugel finite element $P_{BR}(K)$ see [23], which is the less expensive element and when associated with the space of piecewise constant pressures, leads to an optimal inf–sup condition on Ω_F.

$$X_{nh}^F = \left\{ \boldsymbol{v}_h \in H^1(\Omega_F)^d;\ \forall K \in \mathcal{T}_{nh}^F,\ \boldsymbol{v}_h\big|_K \in P_{BR}(K) \right\},$$
$$P_{BR}(K) = P_1(K)^d \oplus \text{Span}\{\psi_e \boldsymbol{n}_e\}^{d+1},$$

where for each edge ($d = 2$) or face ($d = 3$) e of K, ψ_e denoted the bubble function on e equal to the product of the barycentric coordinates associated with the endpoints or vertices of e, and $\boldsymbol{n}_e$ stands for the unit outward normal vector on e. We also need the space

$$X_{0nh}^F = \left\{ \boldsymbol{v}_h \in X_{nh}^F;\ \boldsymbol{v}_h = 0 \text{ on } \Gamma_F \right\}.$$

We introduce the Bernardi–Raugel operator denoted by Π_{nh}^{BR}:

For any continuous function $\boldsymbol{v}$ on $\overline{\Omega}_F$, the quantity $\Pi_{nh}^{BR}\boldsymbol{v}$ belongs to X_{nh}^F and is defined in a unique way, (see [23, Lemma II.1]) by

$$\begin{cases} \Pi_{nh}^{BR}\boldsymbol{v} = \boldsymbol{v}(\boldsymbol{a}), \\ \displaystyle\int_e (\Pi_{nh}^{BR}\boldsymbol{v} \cdot \boldsymbol{n})(\tau)\, d\tau = \int_e (\boldsymbol{v} \cdot \boldsymbol{n})(\tau)\, d\tau, \end{cases}$$

where $\boldsymbol{a}$ any vertex and e all edges ($d = 2$) or faces ($d = 3$) of elements of $\mathcal{T}_{nh}^F$.

Now for simplicity we consider the operator Π_{nh}:

For any smooth enough function $\boldsymbol{v}$ on Ω_P which is continuous on $\overline{\Omega}_F$, $\Pi_{nh}\boldsymbol{v}$ is equal to $\Pi_{nh}^{BR}\boldsymbol{v}$ on Ω_F and to $\Pi_{nh}^{RT}\boldsymbol{v}$ on Ω_P.

We define the discrete space of pressures as

$$\mathbb{M}_{nh} = \left\{ q_h \in L^2(\Omega);\ \forall K \in \mathcal{T}_{nh},\ q_h\big|_K \in P_0(K) \right\}.$$

Remark 3. In dimension $d = 2$, piecewise quadratic velocities can also be used on Ω_F and in dimension $d = 3$, $P_{BR}(K)$ can be replaced by the space spanned by affine functions and the ψ_e, up to the power d.

On Γ, we define the space see [34, Sec. 3]

$$\mathbb{W}_{nh} = \left\{ \varphi_h \in L^2(\Gamma);\ \forall e \in \mathcal{E}_{nh}^{P,\Gamma},\ \varphi_h\Big|_e \in P_0(e) \right\}.$$

The global spaces of velocity are then the spaces $\mathbb{X}_{nh}$ and $\mathbb{X}_{0nh}$ of functions $\boldsymbol{v}_h$ such that

- their restrictions $\boldsymbol{v}_h|_{\Omega_P}$ to Ω_P belongs to X_{nh}^P and X_{0nh}^P, respectively;
- their restrictions $\boldsymbol{v}_h|_{\Omega_F}$ to Ω_F belongs to X_{nh}^F and X_{0nh}^F, respectively;
- the following matching conditions hold on Γ see [39] and [21, Sec. 4]

$$\forall \varphi_h \in \mathbb{W}_{nh}, \quad \int_\Gamma ((\boldsymbol{v}_h|_{\Omega_P} - \boldsymbol{v}_h|_{\Omega_F}) \cdot \boldsymbol{n})(\tau)\, \varphi_h(\tau)\, d\tau = 0. \tag{27}$$

These conditions are not sufficient to enforce the continuity of $\boldsymbol{v}_h \cdot \boldsymbol{n}$ through Γ, so that the discretization is nonconforming: For instance, $\mathbb{X}_{nh}$ is not contained in $H(\text{div}, \Omega)$. However, the spaces $\mathbb{X}_{nh}$ and $\mathbb{X}_{0nh}$ are still equipped with the norm $\|\cdot\|_{X(\Omega)}$.

To discretize the boundary conditions that appear in (22), we denote by k_h^n the piecewise constant approximation of $k^n = k(\cdot, t_n)$ defined by

$$\forall K \in \mathcal{T}_{nh}^P / \text{mes}(K \cap \Gamma_P) > 0,\ k_h^n|_{K\cap\Gamma_P} = \frac{1}{\text{mes}(K \cap \Gamma_P)} \int_{K\cap\Gamma_P} k^n(\tau)\, d\tau,$$

Note that this choice requires that $k^n = k(\cdot, t_n)$ belongs to $\mathcal{C}^0(0, T; H^{-\sigma}(\Omega))$, $\sigma < \frac{1}{2}$. We also introduce an approximation of $\boldsymbol{g}^n = \boldsymbol{g} = (\cdot, t_n)$: When $\boldsymbol{g}^n$ is continuous on $\overline{\Gamma}_F$ (which is slightly stronger than the hypothesis made in (6)), the function $\boldsymbol{g}_h^n$ approximation of $\boldsymbol{g}^n$ belongs to the trace space of X_{nh}^F and satisfies:

For each $K \in \mathcal{T}_{nh}^F$, $\boldsymbol{g}_h^n(\boldsymbol{a}) = \boldsymbol{g}^n(\boldsymbol{a})$ for each endpoint or vertex $\boldsymbol{a}$ of $K \cap \Gamma_F$, and

$$\int_{K\cap\Gamma_F} (\boldsymbol{g}_h^n \cdot \boldsymbol{n})(\tau)\, d\tau = \int_{K\cap\Gamma_F} (\boldsymbol{g}^n \cdot \boldsymbol{n})(\tau)\, d\tau.$$

These conditions define k_h^n and $\boldsymbol{g}_h^n$ in a unique way, see [24, Rem. 3] and [23, Lem. II.1].

Now, we can write the fully discrete problem constructed from problem (21)–(22)–(23) by the Galerkin method. For this, we assume that the data

$$\begin{aligned} &\boldsymbol{f} \in \mathcal{C}^0(0, T; L^2(\Omega)^d),\ k \in \mathcal{C}^0(0, T; H^{\sigma_P}(\Gamma_P)),\ p_a \in \mathcal{C}^0(0, T; H_{00}^{\frac{1}{2}}(\Gamma_{aP})),\\ &\boldsymbol{g} \in \mathcal{C}^0(0, T; H^{\sigma_F}(\Gamma_F)^d), \boldsymbol{t}_a \in \mathcal{C}^0(0, T; H^{-\frac{1}{2}}(\Gamma_{aF})^d),\\ &\sigma_P > -\frac{1}{2}, \sigma_F > \frac{d-1}{2} \text{ and } \boldsymbol{u}^0 \in X(\Omega). \end{aligned} \tag{28}$$

Then the discrete problem reads:

Find $(\boldsymbol{u}_h^n)_{0\le n\le N}$ in $(\mathbb{X}_{nh})^{N+1}$ and $(p_h^n)_{1\le n\le N}$ in $(\mathbb{M}_{nh})^N$ such that

$$\boldsymbol{u}_h^0 = \Pi_{0h}\boldsymbol{u}^0 \quad \text{in } \Omega, \tag{29}$$

such that, for all n, $1 \le n \le N$,

$$\boldsymbol{u}_h^n \,.\, \boldsymbol{n} = k_h^n \quad \text{on } \Gamma_P, \quad \text{and} \quad \boldsymbol{u}_h^n = \boldsymbol{g}_h^n \quad \text{on } \Gamma_F, \tag{30}$$

$$\forall \boldsymbol{v}_h \in \mathbb{X}_{0nh}, \quad (\boldsymbol{u}_h^n, \boldsymbol{v}_h) + \tau_n a(\boldsymbol{u}_h^n, \boldsymbol{v}_h) + \tau_n b(\boldsymbol{v}_h, p_h^n) = (\boldsymbol{u}_h^{n-1}, \boldsymbol{v}_h) + \tau_n \mathcal{L}^n(\boldsymbol{v}_h), \tag{31}$$

$\forall\, q_h \in \mathbb{M}_{nh}, \quad b(\boldsymbol{u}_h^n, q_h) = 0.$

Recalling the main results concerning this problem, see [25] and also [5, Lems. 3.11 and 3.13] which are proven:
(i) If Γ_F has a positive measure in $\partial\Omega_F$, then the following property holds for $\alpha_* = \min(\alpha, \nu) > 0$

$$\forall \boldsymbol{v}_h \in \mathbb{V}_{nh}, \quad \alpha_* \, \|\boldsymbol{v}_h\|_{X(\Omega)}^2 \lesssim a(\boldsymbol{v}_h, \boldsymbol{v}_h). \tag{32}$$

(ii) There exists a positive constant β, independent of h, such that

$$\forall q_h \in \mathbb{M}_{nh}, \quad \sup_{\boldsymbol{v}_h \in \mathbb{X}_{0nh}} \frac{b(\boldsymbol{v}_h, q_h)}{\|\boldsymbol{v}_h\|_{X(\Omega)}} \ge \beta \, \|q_h\|_{L^2(\Omega)}. \tag{33}$$

Let also introduce the discrete kernel:

$$\mathbb{V}_{nh} = \{\boldsymbol{v}_h \in \mathbb{X}_{0nh};\ \forall q_h \in \mathbb{M}_{nh},\ b(\boldsymbol{v}_h, q_h) = 0\}. \tag{34}$$

The functions in $\mathbb{V}_{nh}$ are divergence-free only on Ω_P.

Analogous to previous and in the case $\boldsymbol{t}_a = k = \boldsymbol{g} = 0$, we will find a new variational formulation which is equivalent to problem (29)–(30)–(31).

For this, we set: $p_{*h}^n = p_h^n - \tilde{p}_{ah}^n$, where $\tilde{p}_{ah}^n$ is a piecewise constant, approximation of $\tilde{p}_a^n$ (introduced in (24)), satisfies $\tilde{p}_{ah}^n = p_h^n$ on Γ_{aP} and vanishes on $\partial\Omega \setminus \Gamma_{aP}$.

This leads to consider the problem:

Find $(\boldsymbol{u}_h^n)_{0\le n\le N}$ in $(\mathbb{X}_{0nh})^{N+1}$ and $(p_{*h}^n)_{1\le n\le N}$ in $(\mathbb{M}_{nh})^N$, satisfying

$$\boldsymbol{u}_h^0 = \Pi_{0h}\boldsymbol{u}^0 \quad \text{in} \quad \Omega, \tag{35}$$

and such that, for $1 \le n \le N$,

$$\begin{aligned} &\forall \boldsymbol{v}_h \in \mathbb{X}_{0nh}, \quad (\boldsymbol{u}_h^n - \boldsymbol{u}_h^{n-1}, \boldsymbol{v}_h) + \tau_n a(\boldsymbol{u}_h^n, \boldsymbol{v}_h) + \tau_n b(\boldsymbol{v}_h, p_{*h}^n) = \tau_n L^n(\boldsymbol{v}_h),\\ &\forall\, q_h \in \mathbb{M}_{nh}, \quad b(\boldsymbol{u}_h^n, q_h) = 0, \end{aligned} \tag{36}$$

where, $L^n(\boldsymbol{v}) = L(\cdot, t_n)(\boldsymbol{v}) = (\boldsymbol{f}^n, \boldsymbol{v}) - (\nabla\tilde{p}_a^n, \boldsymbol{v})$ (L is defined in (18)).

The following existence and stability results can be derived from [25, Sec. 3.3, Thm. 4].

Theorem 2. *Assume that Γ_F has a positive measure in $\partial\Omega_F$ and $\boldsymbol{t}_a = k = \boldsymbol{g} = 0$. Then, for any data $(\boldsymbol{f}, p_a, \boldsymbol{u}^0)$ satisfying (28), problem (29)–(30)–(31) has a unique solution $(\boldsymbol{u}_h^n, p_h^n)$ such that*

$$\boldsymbol{u}_h^n \in \mathbb{X}_{nh}, \quad 0 \le n \le N, \quad \text{and} \quad p_h^n \in \mathbb{M}_{nh}, \quad 1 \le n \le N.$$

Moreover, this solution satisfies

$$\Big(\|\boldsymbol{u}_h^n\|^2_{L^2(\Omega)^d} + \alpha_* \sum_{m=1}^{n} \tau_m \, \|\boldsymbol{u}_h^m\|^2_{X(\Omega)} \Big)^{\frac{1}{2}} \lesssim \|\Pi_{0h}\boldsymbol{u}^0\|_{X(\Omega)}$$
$$+ \frac{1}{\sqrt{\alpha_*}} \Big(\sum_{m=1}^{n} \tau_m \big(\|\boldsymbol{f}^m\|^2_{L^2(\Omega)^d} + \|p_a^m\|^2_{H^{\frac{1}{2}}_{00}(\Gamma_{aP})} \big) \Big)^{\frac{1}{2}}. \tag{37}$$

3. A posteriori analysis of the time discretization

For the time discretization, we define the following time error indicator and prove upper and lower bounds for the error. For each n, $1 \le n \le N$,

$$\eta_n = \Big(\frac{\tau_n}{3}\Big)^{\frac{1}{2}} \, \|\boldsymbol{u}_h^n - \boldsymbol{u}_h^{n-1}\|_{X(\Omega)}. \tag{38}$$

We refer to [40] for the first idea of this type of indicators and to [32] for its use in the a posteriori analysis of the heat equation.

Let $\boldsymbol{u}_\tau$ denotes the function which is continuous, affine on each interval $[t_{n-1}, t_n]$, $1 \le n \le N$, which take in the interval $[t_{n-1}, t_n]$ the values

$$\boldsymbol{u}_\tau(t) = \frac{t - t_{n-1}}{\tau_n}(\boldsymbol{u}^n - \boldsymbol{u}^{n-1}) + \boldsymbol{u}^{n-1} = -\frac{t_n - t}{\tau_n}(\boldsymbol{u}^n - \boldsymbol{u}^{n-1}) + \boldsymbol{u}^n,$$

and p_τ denotes the piecewise constant function such that

$$\forall n,\ 1 \le n \le N, \quad \forall t \in]t_{n-1}, t_n], \quad p_\tau(t) = p(t_n).$$

All this leads to the following residual equation in variational form: Since the solution of problem (16)–(17) is divergence-free, the solutions of problems (16)–(17) and (25)–(26) verify for t in $]t_{n-1}, t_n]$

$$(\boldsymbol{u} - \boldsymbol{u}_\tau)(\cdot, 0) = 0 \quad \text{in } \Omega, \tag{39}$$

$$\forall \boldsymbol{v} \in X_0(\Omega), \quad (\partial_t(\boldsymbol{u} - \boldsymbol{u}_\tau), \boldsymbol{v}) + a(\boldsymbol{u} - \boldsymbol{u}_\tau, \boldsymbol{v}) + b(\boldsymbol{v}, p_* - \Pi_\tau p_{*\tau})$$
$$= (L(\cdot, t) - L^n)(\boldsymbol{v}) - a(\boldsymbol{u}_\tau - \boldsymbol{u}^n, \boldsymbol{v}), \tag{40}$$

$$\forall q \in L^2(\Omega), \quad b(\boldsymbol{u} - \boldsymbol{u}_\tau, q) = 0,$$

where Π_τ denotes the operator which associates with any continuous function $\boldsymbol{v} \in [0, T]$, the constant function $\Pi_\tau \boldsymbol{v}$ equal to $\boldsymbol{v}(t_n)$ on each interval $]t_{n-1}, t_n]$, $1 \le n \le N$. Let the regularity parameter

$$\sigma_\tau = \max_{1 \le n \le N} \frac{\tau_n}{\tau_{n-1}},$$

where we have set $\tau_0 = \tau_1$ for the sake of simplicity.

3.1. The reliability of the indicator

Proposition 2. *The following a posteriori error estimate holds, for* $1 \le n \le N$,

$$\|(\boldsymbol{u} - \boldsymbol{u}_\tau)(\cdot, t_n)\|^2_{L^2(\Omega)^d} + \alpha_* \, \|\boldsymbol{u} - \boldsymbol{u}_\tau\|^2_{L^2(0,t_n;X(\Omega))}$$
$$\lesssim \frac{1}{\alpha_*} \Big(\epsilon_D^2 + \sum_{m=1}^{n} \eta_m^2 + (1 + \sigma_\tau) \sum_{m=0}^{n} \tau_m \, \|\boldsymbol{u}^m - \boldsymbol{u}_h^m\|^2_{X(\Omega)} \Big), \tag{41}$$

where

$$\epsilon_D^2 = \|\boldsymbol{f} - \Pi_\tau \boldsymbol{f}\|^2_{L^2(0,t_n;L^2(\Omega)^d)} + \|p_a - \Pi_\tau p_a\|^2_{L^2(0,t_n;H^{\frac{1}{2}}_{00}(\Gamma_{aP}))}.$$

Proof. Taking $\boldsymbol{v} = \boldsymbol{u} - \boldsymbol{u}_\tau$ in the first equation of (40) and $q = p_* - \Pi_\tau p_{*\tau}$ in the second equation, we obtain

$$\frac{d}{dt} \|\boldsymbol{u} - \boldsymbol{u}_\tau\|^2_{L^2(\Omega)^d} + \alpha_* \, \|\boldsymbol{u} - \boldsymbol{u}_\tau\|^2_{X(\Omega)} \lesssim \frac{1}{\alpha_*}(\|\boldsymbol{u}_\tau - \Pi_\tau \boldsymbol{u}_\tau\|^2_{X(\Omega)} + \|\boldsymbol{f} - \Pi_\tau \boldsymbol{f}\|^2_{L^2(\Omega)^d}$$
$$+ \|p_a - \Pi_\tau p_a\|^2_{H^{\frac{1}{2}}_{00}(\Gamma_{aP})}).$$

Integrating this inequality between 0 and t_n yields

$$\|(\boldsymbol{u}-\boldsymbol{u}_\tau)(\cdot,t_n)\|^2_{L^2(\Omega)^d}+\alpha_*\,\|\boldsymbol{u}-\boldsymbol{u}_\tau\|^2_{L^2(0,t_n;X(\Omega))}$$
$$\lesssim \frac{1}{\alpha_*}(\|\boldsymbol{u}_\tau-\Pi_\tau\boldsymbol{u}_\tau\|^2_{L^2(0,t_n;X(\Omega))}+\epsilon_D^2). \tag{42}$$

To evaluate the first term in the right-hand side, we observe that, on the interval $]t_{n-1},t_n]$,

$$(\boldsymbol{u}_\tau-\Pi_\tau\boldsymbol{u}_\tau)(t)=-\frac{t_n-t}{\tau_n}(\boldsymbol{u}^n-\boldsymbol{u}^{n-1}).$$

Thus by integrating this equation between t_{n-1} and t_n and using the fact that $\tau_n=t_n-t_{n-1}$, we obtain

$$\|\boldsymbol{u}_\tau-\Pi_\tau\boldsymbol{u}_\tau\|_{L^2(t_{n-1},t_n;X(\Omega))}=\left(\frac{\tau_n}{3}\right)^{\frac12}\left\|\boldsymbol{u}^n-\boldsymbol{u}^{n-1}\right\|_{X(\Omega)}. \tag{43}$$

On the other hand, the triangle inequality and the expression of the error indicator (38) yield

$$\left(\frac{\tau_n}{3}\right)^{\frac12}\left\|\boldsymbol{u}^n-\boldsymbol{u}^{n-1}\right\|_{X(\Omega)}\le\left(\frac{\tau_n}{3}\right)^{\frac12}\left\|\boldsymbol{u}^n-\boldsymbol{u}_h^n\right\|_{X(\Omega)}+\eta_n$$
$$+\left(\frac{\tau_n}{3}\right)^{\frac12}\left\|\boldsymbol{u}_h^{n-1}-\boldsymbol{u}^{n-1}\right\|_{X(\Omega)}.$$

Thus we obtain

$$\|\boldsymbol{u}_\tau-\Pi_\tau\boldsymbol{u}_\tau\|_{L^2(t_{n-1},t_n;X(\Omega))}\le\left(\frac{\tau_n}{3}\right)^{\frac12}\left\|\boldsymbol{u}^n-\boldsymbol{u}_h^n\right\|_{X(\Omega)}+\eta_n$$
$$+\left(\frac{\tau_{n-1}}{3}\right)^{\frac12}(\sigma_\tau)^{\frac12}\left\|\boldsymbol{u}_h^{n-1}-\boldsymbol{u}^{n-1}\right\|_{X(\Omega)}.$$

Summing over n with $1\le n\le N$ the square of this inequality, we obtain

$$\|\boldsymbol{u}_\tau-\Pi_\tau\boldsymbol{u}_\tau\|^2_{L^2(0,t_n;X(\Omega))}\lesssim\sum_{m=1}^{n}\eta_m^2+(1+\sigma_\tau)\sum_{m=0}^{n}\tau_m\left\|\boldsymbol{u}^m-\boldsymbol{u}_h^m\right\|^2_{X(\Omega)}. \tag{44}$$

Finally by substituting (44) in (42) we obtain the desired a posteriori error estimate. □

Proposition 3. *The following a posteriori error estimate holds, for* $1\le n\le N$,

$$\|\boldsymbol{u}-\boldsymbol{u}_\tau\|^2_{H^1(0,t_n;L^2(\Omega)^d)}+\alpha_*\,\|(\boldsymbol{u}-\boldsymbol{u}_\tau)(\cdot,t_n)\|^2_{L^2(\Omega)^d}$$
$$\lesssim\sum_{m=1}^{n}\eta_m^2+(1+\sigma_\tau)\sum_{m=0}^{n}\tau_m\left\|\boldsymbol{u}^m-\boldsymbol{u}_h^m\right\|^2_{X(\Omega)}.+\epsilon_D^2. \tag{45}$$

Proof. We take $\boldsymbol{v}$ equal to $\partial_t(\boldsymbol{u}-\boldsymbol{u}_\tau)$ in (40) and apply the Cauchy–Schwarz inequality we obtain

$$\frac12\|\partial_t(\boldsymbol{u}-\boldsymbol{u}_\tau)\|^2_{L^2(\Omega)^d}+\frac{\alpha}{2}\frac{d}{dt}\|\boldsymbol{u}-\boldsymbol{u}_\tau\|^2_{L^2(\Omega_P)^d}+\frac{\nu}{2}\frac{d}{dt}|\boldsymbol{u}-\boldsymbol{u}_\tau|^2_{H^1(\Omega_F)^d}$$
$$\le\|\boldsymbol{f}-\Pi_\tau\boldsymbol{f}\|^2_{L^2(\Omega)^d}+\|p_a-\Pi_\tau p_a\|^2_{H^{\frac12}_{00}(\Gamma_{aP})}+\|\boldsymbol{u}_\tau-\Pi_\tau\boldsymbol{u}_\tau\|^2_{X(\Omega)}.$$

Integrating between 0 and t_n, using the fact that $\alpha_*=\min(\alpha,\nu)$ and $(\boldsymbol{u}-\boldsymbol{u}_\tau)(0)=0$, yield

$$\|\partial_t(\boldsymbol{u}-\boldsymbol{u}_\tau)\|^2_{L^2(0,t_n;L^2(\Omega)^d)}+\alpha_*\,\|(\boldsymbol{u}-\boldsymbol{u}_\tau)(\cdot,t_n)\|^2_{L^2(\Omega)^d}$$
$$\lesssim\epsilon_D^2+\|\boldsymbol{u}_\tau-\Pi_\tau\boldsymbol{u}_\tau\|^2_{L^2(0,t_n;X(\Omega))}.$$

Finally, by substituting (44) in this estimate, we obtain the desired estimate. □

Proposition 4. *The following a posteriori error estimate holds, for* $1\le n\le N$,

$$\|p-\Pi_\tau p_\tau\|^2_{L^2(0,t_n;L^2(\Omega))}\lesssim\Big(2+\frac{1}{\alpha_*^2}\Big)\Big(\sum_{m=1}^{n}\eta_m^2+(1+\sigma_\tau)\sum_{m=0}^{n}\tau_m\left\|\boldsymbol{u}^m-\boldsymbol{u}_h^m\right\|^2_{X(\Omega)}+\epsilon_D^2\Big).$$

Proof. From Eq. (40) we have

$$\forall\boldsymbol{v}\in X_0(\Omega),\ b(\boldsymbol{v},p_*-\Pi_\tau p_{*\tau})=(L(\cdot,t)-L^n)(\boldsymbol{v})-(\partial_t(\boldsymbol{u}-\boldsymbol{u}_\tau),\boldsymbol{v})-a(\boldsymbol{u}-\boldsymbol{u}_\tau,\boldsymbol{v})-\ a(\boldsymbol{u}_\tau-\boldsymbol{u}^n,\boldsymbol{v}).$$

The Cauchy–Schwarz inequality and the inf–sup (13) condition yield

$$\|p_* - \Pi_\tau p_{*\tau}\|_{L^2(\Omega)} \lesssim \|\boldsymbol{f} - \Pi_\tau \boldsymbol{f}\|_{L^2(\Omega)^d} + \|p_a - \Pi_\tau p_a\|_{H^{\frac{1}{2}}_{00}(\Gamma_{aP})}$$
$$+ \|\partial_t(\boldsymbol{u} - \boldsymbol{u}_\tau)\|_{L^2(\Omega)^d} + \|\boldsymbol{u} - \boldsymbol{u}_\tau\|_{X(\Omega)} + \|\boldsymbol{u}_\tau - \Pi_\tau \boldsymbol{u}_\tau\|_{X(\Omega)}.$$

Integrating between 0 and t_n we obtain

$$\|p_* - \Pi_\tau p_{*\tau}\|^2_{L^2(0,t_n;L^2(\Omega))} \lesssim \epsilon_D^2 + \|\boldsymbol{u} - \boldsymbol{u}_\tau\|^2_{H^1(0,t_n;L^2(\Omega)^d)}$$
$$+ \|\boldsymbol{u} - \boldsymbol{u}_\tau\|^2_{L^2(0,t_n;X(\Omega))} + \|\boldsymbol{u}_\tau - \Pi_\tau \boldsymbol{u}_\tau\|^2_{L^2(0,t_n;X(\Omega))}.$$

Finally from (41), (44), (45), the fact that $p_* = p - \tilde{p}_a$, $p_*^n = p^n - \tilde{p}_a^n$ and the triangle inequality we obtain the desired a posteriori estimate. □

Corollary 1. *The following a posteriori error estimate holds, for* $1 \le n \le N$,

$$\|\boldsymbol{u} - \boldsymbol{u}_\tau\|^2_{H^1(0,t_n;L^2(\Omega)^d)} + \alpha_* \|\boldsymbol{u} - \boldsymbol{u}_\tau\|^2_{L^2(0,t_n;X(\Omega))} + \|p - \Pi_\tau p_\tau\|^2_{L^2(0,t_n;L^2(\Omega))}$$
$$\lesssim \Big(3 + \frac{1}{\alpha_*^2} + \frac{1}{\alpha_*}\Big)\Big(\epsilon_D^2 + \sum_{m=1}^{n} \eta_m^2 + \sum_{m=0}^{n} \tau_m (1+\sigma_\tau) \left\|\boldsymbol{u}^m - \boldsymbol{u}_h^m\right\|^2_{X(\Omega)}\Big). \tag{46}$$

The last term in (46) and (41), will be evaluated afterward.

3.2. The efficiency of the indicator

We now establish the upper bound for each indicator η_n.

Proposition 5. *Each indicator* η_n, *for* $1 \le n \le N$, *defined in* (38) *satisfies the following bound*

$$\eta_n \lesssim (1 + \sqrt{\sigma_\tau})\Big(\sum_{m=n-1}^{n} \tau_m \left\|\boldsymbol{u}^m - \boldsymbol{u}_h^m\right\|^2_{X(\Omega)}\Big)^{\frac{1}{2}}$$
$$+ \frac{1}{\alpha_*}\Big(\|\boldsymbol{f} - \Pi_\tau \boldsymbol{f}\|_{L^2(t_{n-1},t_n;L^2(\Omega)^d)} + \|p_a - \Pi_\tau p_a\|_{L^2(t_{n-1},t_n;H^{\frac{1}{2}}_{00}(\Gamma_{aP}))}$$
$$+ \|\boldsymbol{u} - \boldsymbol{u}_\tau\|_{H^1(t_{n-1},t_n;L^2(\Omega)^d)} + \|\boldsymbol{u} - \boldsymbol{u}_\tau\|_{L^2(t_{n-1},t_n;X(\Omega))}$$
$$+ \|p - \Pi_\tau p_\tau\|_{L^2(t_{n-1},t_n;L^2(\Omega))}\Big).$$

Proof. Thanks to the triangle inequality, we have

$$\eta_n \le \Big(\frac{\tau_n}{3}\Big)^{\frac{1}{2}} \left\|\boldsymbol{u}^n - \boldsymbol{u}^{n-1}\right\|_{X(\Omega)} + \Big(\frac{\tau_n}{3}\Big)^{\frac{1}{2}} \left\|\boldsymbol{u}^n - \boldsymbol{u}_h^n\right\|_{X(\Omega)}$$
$$+ \Big(\frac{\tau_{n-1}}{3}\Big)^{\frac{1}{2}} (\sigma_\tau)^{\frac{1}{2}} \left\|\boldsymbol{u}^{n-1} - \boldsymbol{u}_h^{n-1}\right\|_{X(\Omega)},$$

then,

$$\eta_n \lesssim (\frac{\tau_n}{3})^{\frac{1}{2}} \left\|\boldsymbol{u}^n - \boldsymbol{u}^{n-1}\right\|_{X(\Omega)} + (1 + \sqrt{\sigma_\tau})\Big(\sum_{m=n-1}^{n} \tau_m \left\|\boldsymbol{u}^m - \boldsymbol{u}_h^m\right\|^2_{X(\Omega)}\Big)^{\frac{1}{2}}.$$

In order to bound the first term, we take $\boldsymbol{v} = \boldsymbol{u}^n - \boldsymbol{u}_\tau(t)$ in the first line of (40). This gives

$$\int_{t_{n-1}}^{t_n} \left\|(\boldsymbol{u}^n - \boldsymbol{u}_\tau)(\cdot, s)\right\|^2_{X(\Omega)} ds \lesssim \frac{1}{\alpha_*}\Big(\|\boldsymbol{f} - \Pi_\tau \boldsymbol{f}\|_{L^2(t_{n-1},t_n;L^2(\Omega)^d)}$$
$$+ \|p_a - \Pi_\tau p_a\|_{L^2(t_{n-1},t_n;H^{\frac{1}{2}}_{00}(\Gamma_{aP}))} + \|\boldsymbol{u} - \boldsymbol{u}_\tau\|_{H^1(t_{n-1},t_n;L^2(\Omega)^d)}$$
$$+ \|\boldsymbol{u} - \boldsymbol{u}_\tau\|_{L^2(t_{n-1},t_n;X(\Omega))} + \|p_* - \Pi_\tau p_{*\tau}\|_{L^2(t_{n-1},t_n;L^2(\Omega))}\Big)$$
$$\Big(\int_{t_{n-1}}^{t_n} \left\|(\boldsymbol{u}^n - \boldsymbol{u}_\tau)(\cdot, s)\right\|^2_{X(\Omega)} ds\Big)^{\frac{1}{2}},$$

or equivalently, from (43)

$$\left(\frac{\tau_n}{3}\right)^{\frac{1}{2}} \|\boldsymbol{u}^n - \boldsymbol{u}^{n-1}\|_{X(\Omega)} \lesssim \frac{1}{\alpha_*}\Big(\|\boldsymbol{f} - \Pi_\tau \boldsymbol{f}\|_{L^2(t_{n-1},t_n;L^2(\Omega)^d)} + \|p_a - \Pi_\tau p_a\|_{L^2(t_{n-1},t_n;H_{00}^{\frac{1}{2}}(\Gamma_{aP}))} + \|\boldsymbol{u} - \boldsymbol{u}_\tau\|_{H^1(t_{n-1},t_n;L^2(\Omega)^d)} + \|\boldsymbol{u} - \boldsymbol{u}_\tau\|_{L^2(t_{n-1},t_n;X(\Omega))} + \|p_* - \Pi_\tau p_{*\tau}\|_{L^2(t_{n-1},t_n;L^2(\Omega))}\Big).$$

The fact that $p_* = p - \tilde{p}_a$, $p_*^n = p^n - \tilde{p}_a^n$ and the triangle inequality give the desired result. □

4. A posteriori analysis of the space discretization

In order to describe the family of space error indicators, we need some notations.

For each n and each K in $\mathcal{T}_{nh}^P$, we introduce
- $\mathcal{E}_K$ the set of edges ($d = 2$) or faces ($d = 3$) of K which are not contained in $\partial\Omega_P$,
- $\mathcal{E}_K^{aP}$ the set of edges ($d = 2$) or faces ($d = 3$) of K which are contained in $\overline{\Gamma}_{aP}$.

For each n and each K in $\mathcal{T}_{nh}^F$, we introduce
- $\mathcal{E}_K$ the set of edges ($d = 2$) or faces ($d = 3$) of K which are not contained in $\partial\Omega_F$,
- $\mathcal{E}_K^{aF}$ the set of edges ($d = 2$) or faces ($d = 3$) of K which are contained in $\overline{\Gamma}_{aF}$.

For each n and each e in any of the $\mathcal{E}_K$ and also in $\mathcal{E}_{nh}^{P,\Gamma}$ ($\mathcal{E}_{nh}^{P,\Gamma}$ is defined in Section 2.3), we agree to denote by $[\cdot]_e$ the jump through e (making its sign precise is not necessary). We also denote by h_e the length ($d = 2$) or diameter ($d = 3$) of e.

We need a further notation for some global sets:
- $\mathcal{E}_{nh}^{aP}$ is the set of edges or faces of elements of $\mathcal{T}_{nh}^P$, which are contained in $\overline{\Gamma}_{aP}$.
- $\mathcal{E}_{nh}^{P}$ is the set of all other edges or faces of elements of $\mathcal{T}_{nh}^P$.

With each element K of $\mathcal{T}_{nh}^F$ and each edge e of K, we associate the quantities γ_K and γ_e equal to 1 if K or e, respectively, intersects $\overline{\Gamma} \setminus \overline{\Gamma}_F$ and to zero otherwise.

We introduce the space $\mathbb{Z}_{nh}$ of functions in $L^2(\Omega)^d$ such that their restrictions to each K in $\mathcal{T}_{nh}^P$ or in $\mathcal{T}_{nh}^F$ is constant. Similarly, we denote by $\mathbb{Z}_{nh}^F$ the space of functions in $L^2(\Gamma_{aF})^d$ such that their restriction to each e in $\mathcal{E}_K^{aF}$, $K \in \mathcal{T}_{nh}^F$, is constant. Indeed, we consider an approximation $\boldsymbol{f}_h^n$ of the data $\boldsymbol{f}^n = \boldsymbol{f}(\cdot, t_n)$ in $\mathbb{Z}_{nh}$ and an approximation $\boldsymbol{t}_{ah}^n$ of $\boldsymbol{t}_a^n = \boldsymbol{t}_a(\cdot, t_n)$ in $\mathbb{Z}_{nh}^F$.

Finally, assuming that the datum $p_a^n = p_a(\cdot, t_n)$ is continuous on $\overline{\Gamma}_{aP}$, we define p_{ah}^n as the function which is affine on each e in $\mathcal{E}_K^{aP}$, $K \in \mathcal{T}_{nh}^P$, and equal to $p_a^n(\boldsymbol{a})$ at all endpoints ($d = 2$) or vertices ($d = 3$) $\boldsymbol{a}$ of these e.

The error indicators are now defined by analogy with the stationary problem, see ([5, Sect. 5]).

- For each n, $1 \le n \le N$, and for each K in $\mathcal{T}_{nh}^P$, the error indicator η_K^{nP} is defined by

$$\eta_K^{nP} = \left\| \boldsymbol{f}_h^n - \frac{\boldsymbol{u}_h^n - \boldsymbol{u}_h^{n-1}}{\tau_n} - \alpha \boldsymbol{u}_h^n \right\|_{L^2(K)^d} + \sum_{e \in \mathcal{E}_K} h_e^{-\frac{1}{2}} \left\| [p_h^n]_e \right\|_{L^2(e)} + \sum_{e \in \mathcal{E}_K^{aP}} h_e^{-\frac{1}{2}} \left\| p_{ah}^n - p_h^n \right\|_{L^2(e)}. \tag{47}$$

- For each n, $1 \le n \le N$, and for each K in $\mathcal{T}_{nh}^F$, the error indicator η_K^{nF} is defined by

$$\eta_K^{nF} = h_K^{1-\gamma_K} \left\| \boldsymbol{f}_h^n - \frac{\boldsymbol{u}_h^n - \boldsymbol{u}_h^{n-1}}{\tau_n} + \nu \Delta \boldsymbol{u}_h^n \right\|_{L^2(K)^d} + \left\| \mathrm{div} \boldsymbol{u}_h^n \right\|_{L^2(K)} + \sum_{e \in \mathcal{E}_K} h_e^{\frac{1}{2}-\gamma_e} \left\| [\nu \partial_n \boldsymbol{u}_h^n - p_h^n \boldsymbol{n}]_e \right\|_{L^2(e)^d} + \sum_{e \in \mathcal{E}_K^{aF}} h_e^{\frac{1}{2}-\gamma_e} \left\| \boldsymbol{t}_{ah}^n - \nu \partial_n \boldsymbol{u}_h^n + p_h^n \boldsymbol{n} \right\|_{L^2(e)^d}. \tag{48}$$

- For each n, $1 \le n \le N$, and for each e in $\mathcal{E}_{nh}^{P,\Gamma}$, the error indicator $\eta_e^{n\Gamma}$ is defined by

$$\eta_e^{n\Gamma} = \left\| (p_h^n \boldsymbol{n})|_{\Omega_P} + (\nu \partial_n \boldsymbol{u}_h^n - p_h^n \boldsymbol{n})|_{\Omega_F} \right\|_{L^2(e)^d} + h_e^{-\frac{1}{2}} \left\| [\boldsymbol{u}_h^n \cdot \boldsymbol{n}]_e \right\|_{L^2(e)}. \tag{49}$$

Remark 4. These indicators are easy to compute once the discrete solution $(\boldsymbol{u}_h^n, p_h^n)$ is known and they are all of residual type. Moreover the second term in the $\eta_e^{n\Gamma}$ comes from the nonconformity of the discretization.

4.1. The residual equation

The function $\boldsymbol{u}^n - \boldsymbol{u}_h^n$ does not belong to $X_0(\Omega)$ and even not to $X(\Omega)$, so that the idea consists in building a conforming approximation of $\boldsymbol{u}_h^n$, namely an approximation which belongs to $X(\Omega)$ (see [34, Lem. 5.4] for a similar argument and [41] for a general analysis in a different context).

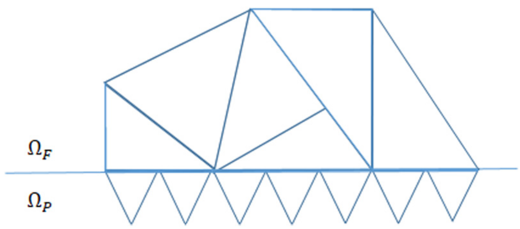

Fig. 2. Illustration of Assumption 4.

We are led to make a further assumption, which is now standard in the a posteriori analysis of mortar element discretizations (and is stronger than Assumption 3). Let us recall that $\mathcal{E}_{nh}^{F,\Gamma}$ and $\mathcal{E}_{nh}^{P,\Gamma}$ are defined in Section 2.3.

Assumption 4. Each element e of $\mathcal{E}_{nh}^{F,\Gamma}$ is the union of a finite number of elements of $\mathcal{E}_{nh}^{P,\Gamma}$, where "finite" means bounded independently of h_P and h_F (see Fig. 2).

Lemma 1. *If Assumption 4 holds, then (see [5, Lem. 5.3]), there exists a finite element function $\boldsymbol{u}_h^{\diamond n} \in X(\Omega)$ satisfying*

$$\boldsymbol{u}_h^{\diamond n} \,.\, \boldsymbol{n} = 0 \quad \text{on } \Gamma_P, \quad \boldsymbol{u}_h^{\diamond n} = 0 \quad \text{on } \Gamma_F,$$

and

$$\|\boldsymbol{u}_h^n - \boldsymbol{u}_h^{\diamond n}\|_{X(\Omega)} \lesssim \Big(\sum_{e\in\mathcal{E}_{nh}^{P,\Gamma}} h_e^{-1} \, \|[\boldsymbol{u}_h^n \cdot \boldsymbol{n}]_e\|_{L^2(e)}^2 \Big)^{\frac{1}{2}}. \tag{50}$$

For a different reason, mainly due to the lack of regularity of the normal trace of functions in $H(\mathrm{div}, \Omega_P)$, we also need an approximation $p_h^{\diamond n}$ of p_h^n in $H^1(\Omega_P)$. The construction of such a function is standard, see [42, Thm. 4.7].

Lemma 2. *There exists a finite element function $p_h^{\diamond n}$ equal to p_h^n on Ω_F and to p_{ah}^n on Γ_{aP} such that $p_h^{\diamond n}|_{\Omega_P} \in H^1(\Omega_P)$ and satisfies*

$$\|p_h^n - p_h^{\diamond n}\|_{L^2(\Omega_P)} \lesssim \Big(\sum_{e\in\mathcal{E}_{nh}^{P}} h_e \, \|[p_h^n]_e\|_{L^2(e)}^2 + \sum_{e\in\mathcal{E}_{nh}^{aP}} h_e \, \|p_{ah}^n - p_h^n\|_{L^2(e)}^2 \Big)^{\frac{1}{2}}, \tag{51}$$

$$|p_h^{\diamond n}|_{H^1(\Omega_P)} \lesssim \Big(\sum_{e\in\mathcal{E}_{nh}^{P}} h_e^{-1} \, \|[p_h^n]_e\|_{L^2(e)}^2 + \sum_{e\in\mathcal{E}_{nh}^{aP}} h_e^{-1} \, \|p_{ah}^n - p_h^n\|_{L^2(e)}^2 \Big)^{\frac{1}{2}}, \tag{52}$$

and

$$\|p_h^n - p_h^{\diamond n}\|_{L^2(\Gamma)} \lesssim \Big(\sum_{e\in\mathcal{E}_{nh}^{P}} h_e \, \|[p_h^n]_e\|_{L^2(e)}^2 + \sum_{e\in\mathcal{E}_{nh}^{aP}} h_e \, \|p_{ah}^n - p_h^n\|_{L^2(e)}^2 \Big)^{\frac{1}{2}}. \tag{53}$$

Proof. We will construct $p_h^{\diamond n}$ satisfying the properties stated in the lemma. For this: let $\mathcal{V}_{nh}^P$ the set of all vertices $\boldsymbol{a}$ of all elements $K \in \mathcal{T}_{nh}^P$, and define $p_h^{\diamond n}|_{\Omega_P}$ as the function which is affine on each $K \in \mathcal{T}_{nh}^P$, such that

$$p_h^{\diamond n}|_{\Omega_P} = \begin{cases} p_{ah}^n(\boldsymbol{a}) & \forall \boldsymbol{a} \in \mathcal{V}_{nh}^P \cap \overline{\Gamma}_{aP}, \\ \dfrac{\sum p_h^n|_K(\boldsymbol{a})}{nb(\boldsymbol{a})} & \forall \boldsymbol{a} \in \mathcal{V}_{nh}^P \setminus \overline{\Gamma}_{aP}, \end{cases}$$

where $nb(\boldsymbol{a})$ is the number of all vertices $\boldsymbol{a} \in \mathcal{V}_{nh}^P \setminus \overline{\Gamma}_{aP}$. Then estimates (52) and (53) are derived by exactly the same arguments as in [42, Thm. 4.7] and [34, Lem. 5.4]. □

Lemma 3. *For all $\boldsymbol{v} \in X_0(\Omega)$, there exists a function $\boldsymbol{v}_h \in \mathbb{X}_{0nh} \cap X_0(\Omega)$, such that $(\mathrm{support}(\boldsymbol{v}_h)) \subset \Omega_F$, $\forall K \in \mathcal{T}_{nh}^F$ and all edges ($d = 2$) or faces ($d = 3$) $e \in K$,*

$$h_K^{-1(1-\gamma_K)} \|\boldsymbol{v} - \boldsymbol{v}_h\|_{L^2(K)^d} + h_e^{-1(\frac{1}{2}-\gamma_e)} \|\boldsymbol{v} - \boldsymbol{v}_h\|_{L^2(e)^d} \lesssim \|\boldsymbol{v}_h\|_{H^1(\Delta_K)}, \tag{54}$$

where Δ_K is the union of the elements of $\mathcal{T}_{nh}^F$ that intersects K.

Proof. $\forall \boldsymbol{v} \in X_0(\Omega)$, we associate the function

$$\boldsymbol{v}_h = \begin{cases} \tilde{\mathcal{R}}_h \boldsymbol{v} & \text{on} \quad \Omega_F, \\ 0 & \text{on} \quad \Omega_P, \end{cases}$$

where $\tilde{\mathcal{R}}_h$ stands for the modified Clément operator with values in piecewise affine functions which vanish on $\Gamma_F \cup \Gamma$, see for instance respectively [43, Sect. IX.3, Chap. IX, Sect 3.], for a detailed definition of such an operator and the local approximation properties of the operator $\tilde{\mathcal{R}}_h$. This gives the desired result. □

We are now in position to write the residual equation.

When $\boldsymbol{t}_a = k = \boldsymbol{g} = 0$, we observe that $(\boldsymbol{u}^n, p^n)$ solution of problem (21)–(22)–(23) now belongs to $X_0(\Omega) \times L^2(\Omega)$ and $\mathcal{L}^n(\boldsymbol{v}) = \mathcal{L}(\cdot, t_n)(\boldsymbol{v})$ ($\mathcal{L}$ is defined in (10)) satisfies

$$\mathcal{L}^n(\cdot, t)(\boldsymbol{v}) = \int_\Omega \boldsymbol{f}^n(\boldsymbol{x}, t) \cdot \boldsymbol{v}(\boldsymbol{x})\, d\boldsymbol{x} - \int_{\Gamma_{aP}} (\boldsymbol{v} \cdot \boldsymbol{n})(\tau)\, p_a^n(\boldsymbol{x}, t)(\tau)\, d\tau.$$

When setting $\boldsymbol{U} = (\boldsymbol{u}^n, p^n)$, $\boldsymbol{U}_h = (\boldsymbol{u}_h^n, p_h^n)$ and $\boldsymbol{U}_h^\diamond = (\boldsymbol{u}_h^{\diamond n}, p_h^{\diamond n})$, then $\boldsymbol{U} - \boldsymbol{U}_h^\diamond = (\boldsymbol{u}^n - \boldsymbol{u}_h^{\diamond n}, p^n - p_h^{\diamond n})$ now belongs to $X_0(\Omega) \times L^2(\Omega)$ and from the first equation of (23), we obtain

$$\begin{aligned} &\forall \boldsymbol{V} = (\boldsymbol{v}, q) \in X_0(\Omega) \times L^2(\Omega), \\ &\quad a(\boldsymbol{u}^n - \boldsymbol{u}_h^{\diamond n}, \boldsymbol{v}) + b(\boldsymbol{v}, p^n - p_h^{\diamond n}) + b(\boldsymbol{u}^n - \boldsymbol{u}_h^{\diamond n}, q) + \Big(\frac{(\boldsymbol{u}^n - \boldsymbol{u}_h^{\diamond n}) - (\boldsymbol{u}^{n-1} - \boldsymbol{u}_h^{\diamond n-1})}{\tau_n}, \boldsymbol{v}\Big) \\ &\quad = -a(\boldsymbol{u}_h^{\diamond n}, \boldsymbol{v}) - b(\boldsymbol{v}, p_h^{\diamond n}) - b(\boldsymbol{u}_h^{\diamond n}, q) - \Big(\frac{(\boldsymbol{u}_h^{\diamond n} - \boldsymbol{u}_h^{\diamond n-1})}{\tau_n}, \boldsymbol{v}\Big) + \mathcal{L}^n(\boldsymbol{v}). \end{aligned}$$

Let $\boldsymbol{v}_h$ the approximation of $\boldsymbol{v}$ exhibited in Lemma 3, then

$$\begin{aligned} &a(\boldsymbol{u}^n - \boldsymbol{u}_h^{\diamond n}, \boldsymbol{v}) + b(\boldsymbol{v}, p^n - p_h^{\diamond n}) + b(\boldsymbol{u}^n - \boldsymbol{u}_h^{\diamond n}, q) + \Big(\frac{(\boldsymbol{u}^n - \boldsymbol{u}_h^{\diamond n}) - (\boldsymbol{u}^{n-1} - \boldsymbol{u}_h^{\diamond n-1})}{\tau_n}, \boldsymbol{v}\Big) \\ &\quad = a(\boldsymbol{u}_h^n - \boldsymbol{u}_h^{\diamond n}, \boldsymbol{v}) + b(\boldsymbol{u}_h^n - \boldsymbol{u}_h^{\diamond n}, q) + \Big(\frac{(\boldsymbol{u}_h^n - \boldsymbol{u}_h^{\diamond n}) - (\boldsymbol{u}_h^{n-1} - \boldsymbol{u}_h^{\diamond n-1})}{\tau_n}, \boldsymbol{v}\Big) \\ &\qquad - \Big(\frac{(\boldsymbol{u}_h^n - \boldsymbol{u}_h^{n-1})}{\tau_n}, \boldsymbol{v}\Big) + \mathcal{L}^n(\boldsymbol{v} - \boldsymbol{v}_h) + \mathcal{L}^n(\boldsymbol{v}_h) - a(\boldsymbol{u}_h^n, \boldsymbol{v}) - b(\boldsymbol{v}, p_h^{\diamond n}) - b(\boldsymbol{u}_h^n, q). \end{aligned}$$

By using the first equation of (31) we obtain

$$\begin{aligned} &a(\boldsymbol{u}^n - \boldsymbol{u}_h^{\diamond n}, \boldsymbol{v}) + b(\boldsymbol{v}, p^n - p_h^{\diamond n}) + b(\boldsymbol{u}^n - \boldsymbol{u}_h^{\diamond n}, q) + \Big(\frac{(\boldsymbol{u}^n - \boldsymbol{u}_h^{\diamond n}) - (\boldsymbol{u}^{n-1} - \boldsymbol{u}_h^{\diamond n-1})}{\tau_n}, \boldsymbol{v}\Big) \\ &\quad = a(\boldsymbol{u}_h^n - \boldsymbol{u}_h^{\diamond n}, \boldsymbol{v}) + b(\boldsymbol{u}_h^n - \boldsymbol{u}_h^{\diamond n}, q) + \Big(\frac{(\boldsymbol{u}_h^n - \boldsymbol{u}_h^{\diamond n}) - (\boldsymbol{u}_h^{n-1} - \boldsymbol{u}_h^{\diamond n-1})}{\tau_n}, \boldsymbol{v}\Big) \\ &\qquad + \mathcal{L}^n(\boldsymbol{v} - \boldsymbol{v}_h) - \Big(\frac{(\boldsymbol{u}_h^n - \boldsymbol{u}_h^{n-1})}{\tau_n}, \boldsymbol{v} - \boldsymbol{v}_h\Big) - a(\boldsymbol{u}_h^n, \boldsymbol{v} - \boldsymbol{v}_h) - b(\boldsymbol{u}_h^n, q) + b(\boldsymbol{v}_h, p_h^n) - b(\boldsymbol{v}, p_h^{\diamond n}). \end{aligned}$$

Notting that $b(\boldsymbol{v}_h, p_h^n - p_h^{\diamond n}) = -(\text{div}\boldsymbol{v}_h, p_h^n - p_h^{\diamond n})_{\Omega_P} - (\text{div}\boldsymbol{v}_h, p_h^n - p_h^{\diamond n})_{\Omega_F}$, using the fact that (support$(\boldsymbol{v}_h)$) $\subset \Omega_F$ and $p_h^{\diamond n} = p_h^n$ on Ω_F, then

$$b(\boldsymbol{v}_h, p_h^n - p_h^{\diamond n}) = 0.$$

Therefore,

$$\begin{aligned} &a(\boldsymbol{u}^n - \boldsymbol{u}_h^{\diamond n}, \boldsymbol{v}) + b(\boldsymbol{v}, p^n - p_h^{\diamond n}) + b(\boldsymbol{u}^n - \boldsymbol{u}_h^{\diamond n}, q) + \Big(\frac{(\boldsymbol{u}^n - \boldsymbol{u}_h^{\diamond n}) - (\boldsymbol{u}^{n-1} - \boldsymbol{u}_h^{\diamond n-1})}{\tau_n}, \boldsymbol{v}\Big) \\ &\quad = a(\boldsymbol{u}_h^n - \boldsymbol{u}_h^{\diamond n}, \boldsymbol{v}) + b(\boldsymbol{u}_h^n - \boldsymbol{u}_h^{\diamond n}, q) + \Big(\frac{(\boldsymbol{u}_h^n - \boldsymbol{u}_h^{\diamond n}) - (\boldsymbol{u}_h^{n-1} - \boldsymbol{u}_h^{\diamond n-1})}{\tau_n}, \boldsymbol{v}\Big) \\ &\qquad + \mathcal{L}^n(\boldsymbol{v} - \boldsymbol{v}_h) - \Big(\frac{(\boldsymbol{u}_h^n - \boldsymbol{u}_h^{n-1})}{\tau_n}, \boldsymbol{v} - \boldsymbol{v}_h\Big) - a(\boldsymbol{u}_h^n, \boldsymbol{v} - \boldsymbol{v}_h) - b(\boldsymbol{u}_h^n, q) - b(\boldsymbol{v} - \boldsymbol{v}_h, p_h^{\diamond n}). \end{aligned}$$

Finally, when setting $\boldsymbol{V}_h = (\boldsymbol{v}_h, 0)$, we obtain by integration by parts the following residual equation:

$$\forall \boldsymbol{V} = (\boldsymbol{v}, q) \text{ in } X_0(\Omega) \times L^2(\Omega),$$

$$\begin{aligned} & a(\boldsymbol{u}^n - \boldsymbol{u}_h^{\diamond n}, \boldsymbol{v}) + b(\boldsymbol{v}, p^n - p_h^{\diamond n}) + b(\boldsymbol{u}^n - \boldsymbol{u}_h^{\diamond n}, q) + \Big(\frac{(\boldsymbol{u}^n - \boldsymbol{u}_h^{\diamond n}) - (\boldsymbol{u}^{n-1} - \boldsymbol{u}_h^{\diamond n-1})}{\tau_n}, \boldsymbol{v}\Big) \\ & = a(\boldsymbol{u}_h^n - \boldsymbol{u}_h^{\diamond n}, \boldsymbol{v}) + b(\boldsymbol{u}_h^n - \boldsymbol{u}_h^{\diamond n}, q) + \Big(\frac{(\boldsymbol{u}_h^n - \boldsymbol{u}_h^{\diamond n}) - (\boldsymbol{u}_h^{n-1} - \boldsymbol{u}_h^{\diamond n-1})}{\tau_n}, \boldsymbol{v}\Big) \\ & \quad + \langle \mathcal{R}_P, \boldsymbol{V} - \boldsymbol{V}_h \rangle + \langle \mathcal{R}_F, \boldsymbol{V} - \boldsymbol{V}_h \rangle + \langle \mathcal{R}_\Gamma, \boldsymbol{V} - \boldsymbol{V}_h \rangle + \langle \mathcal{F}, \boldsymbol{V} - \boldsymbol{V}_h \rangle, \end{aligned} \tag{55}$$

where

$$\begin{aligned} \langle \mathcal{R}_P, \boldsymbol{V} \rangle = \sum_{K \in \mathcal{T}_{nh}^P} \Big(& \int_K \Big(\boldsymbol{f}_h^n - \frac{\boldsymbol{u}_h^n - \boldsymbol{u}_h^{n-1}}{\tau_n} - \alpha \boldsymbol{u}_h^n\Big)(\boldsymbol{x}) \cdot \boldsymbol{v}(\boldsymbol{x})\, d\boldsymbol{x} \\ & - \int_K \boldsymbol{v}(\boldsymbol{x}) \cdot (\mathbf{grad} p_h^{\diamond n})(\boldsymbol{x})\, d\boldsymbol{x} \Big), \end{aligned} \tag{56}$$

$$\begin{aligned} \langle \mathcal{R}_F, \boldsymbol{V} \rangle = \sum_{K \in \mathcal{T}_{nh}^F} \Big(& \int_K \Big(\boldsymbol{f}_h^n - \frac{\boldsymbol{u}_h^n - \boldsymbol{u}_h^{n-1}}{\tau_n} + \nu \Delta \boldsymbol{u}_h^n\Big)(\boldsymbol{x}) \cdot \boldsymbol{v}(\boldsymbol{x})\, d\boldsymbol{x} \\ & + \frac{1}{2} \sum_{e \in \mathcal{E}_K} \int_e \boldsymbol{v}(\tau) \cdot [\nu \partial_n \boldsymbol{u}_h^n - p_h^n \boldsymbol{n}]_e(\tau) d\tau \\ & + \sum_{e \in \mathcal{E}_K^{aF}} \int_e \boldsymbol{v}(\tau) \cdot (-\nu \partial_n \boldsymbol{u}_h^n + p_h^n \boldsymbol{n})(\tau) d\tau + \int_K (\mathrm{div} \boldsymbol{u}_h^n)(\boldsymbol{x}) q(\boldsymbol{x}) d\boldsymbol{x} \Big), \end{aligned} \tag{57}$$

$$\begin{aligned} \langle \mathcal{R}_\Gamma, \boldsymbol{V} \rangle = \sum_{e \in \mathcal{E}_K^{P,\Gamma}} \Big(& \int_e \boldsymbol{v}(\tau) \cdot \big((p_h^n \boldsymbol{n})|_{\Omega_P} + (\nu \partial_n \boldsymbol{u}_h^n - p_h^n \boldsymbol{n})|_{\Omega_F}\big)(\tau) d\tau \\ & + \int_\Gamma (\boldsymbol{v} \cdot \boldsymbol{n})(\tau) \big(p_h^{\diamond n}|_{\Omega_P} - p_h^n|_{\Omega_P}\big)(\tau) d\tau \Big), \end{aligned} \tag{58}$$

$$\langle \mathcal{F}, \boldsymbol{V} \rangle = \int_\Omega (\boldsymbol{f}^n - \boldsymbol{f}_h^n)(\boldsymbol{x}) \cdot \boldsymbol{v}(\boldsymbol{x}) d\boldsymbol{x} - \int_{\Gamma_{aP}} (\boldsymbol{v} \cdot \boldsymbol{n})(\tau)(p_a^n - p_{ah}^n)(\tau) d\tau. \tag{59}$$

4.2. The reliability of the indicators

Note that the next estimate is optimal: Up to the terms involving the data, the full error is bounded by a constant times the Hilbertian sum of all indicators.

Theorem 3. *Assume that Γ_F has a positive measure in $\partial\Omega_F$, that Assumption 4 is satisfied, that the datum p_a is continuous on $\overline{\Gamma}_{aP}$ and in the case $\boldsymbol{t}_a = k = \boldsymbol{g} = 0$. Then the following a posteriori error estimate holds between the solution $(\boldsymbol{u}^n, p^n)$ of problem (21)–(22)–(23) and the solution $(\boldsymbol{u}_h^n, p_h^n)$ of problem (29)–(30)–(31)*

$$\begin{aligned} & \sum_{n=0}^N \tau_n \Big(\|p^n - p_h^n\|_{L^2(\Omega)}^2 + \|\boldsymbol{u}^n - \boldsymbol{u}_h^n\|_{X(\Omega)}^2 + \Big\| \frac{(\boldsymbol{u}^n - \boldsymbol{u}_h^n) - (\boldsymbol{u}^{n-1} - \boldsymbol{u}_h^{n-1})}{\tau_n} \Big\|_{L^2(\Omega)^d}^2 \Big) \\ & \lesssim \sum_{n=0}^N \tau_n \Big(\sum_{K \in \mathcal{T}_{nh}^P} (\eta_K^{nP})^2 + \sum_{K \in \mathcal{T}_{nh}^F} (\eta_K^{nF})^2 \Big) + \sum_{n=0}^N \tau_n \, \|p_a^n - p_{ah}^n\|_{H_{00}^{\frac{1}{2}}(\Gamma_{aP})}^2 \\ & \quad + \sum_{n=0}^N \tau_n \, \|\boldsymbol{f}^n - \boldsymbol{f}_h^n\|_{L^2(\Omega_P)^d}^2 + \sum_{n=0}^N \tau_n \Big(\sum_{K \in \mathcal{T}_{nh}^F} h_K^2 \, \|\boldsymbol{f}^n - \boldsymbol{f}_h^n\|_{L^2(K)}^2 \Big) \\ & \quad + \sum_{n=0}^N \Big(\tau_n + \frac{\sigma_\tau}{\tau_{n+1}}\Big) \Big(\sum_{e \in \mathcal{E}_{nh}^{P,\Gamma}} (\eta_e^{n\Gamma})^2 \Big). \end{aligned} \tag{60}$$

Proof. The triangle inequality gives

$$\begin{aligned}
&\|p^n - p_h^n\|_{L^2(\Omega)} + \|\boldsymbol{u}^n - \boldsymbol{u}_h^n\|_{X(\Omega)} + \left\|\frac{(\boldsymbol{u}^n - \boldsymbol{u}_h^n) - (\boldsymbol{u}^{n-1} - \boldsymbol{u}_h^{n-1})}{\tau_n}\right\|_{L^2(\Omega)^d} \\
&\le \|p^n - p_h^{\diamond n}\|_{L^2(\Omega)} + \|\boldsymbol{u}^n - \boldsymbol{u}_h^{\diamond n}\|_{X(\Omega)} + \left\|\frac{(\boldsymbol{u}^n - \boldsymbol{u}_h^{\diamond n}) - (\boldsymbol{u}^{n-1} - \boldsymbol{u}_h^{\diamond n-1})}{\tau_n}\right\|_{X(\Omega)} \\
&\quad + \left\|\frac{(\boldsymbol{u}_h^{\diamond n} - \boldsymbol{u}_h^n) - (\boldsymbol{u}_h^{\diamond n-1} - \boldsymbol{u}_h^{n-1})}{\tau_n}\right\|_{X(\Omega)} + \|p_h^{\diamond n} - p_h^n\|_{L^2(\Omega)} + \|\boldsymbol{u}_h^{\diamond n} - \boldsymbol{u}_h^n\|_{X(\Omega)}.
\end{aligned} \tag{61}$$

From (55), the ellipticity property (11) and the inf–sup condition (13), we obtain

$$\begin{aligned}
&\|p^n - p_h^{\diamond n}\|_{L^2(\Omega)} + \|\boldsymbol{u}^n - \boldsymbol{u}_h^{\diamond n}\|_{X(\Omega)} + \left\|\frac{(\boldsymbol{u}^n - \boldsymbol{u}_h^{\diamond n}) - (\boldsymbol{u}^{n-1} - \boldsymbol{u}_h^{\diamond n-1})}{\tau_n}\right\|_{X(\Omega)} \\
&\lesssim \|\boldsymbol{u}_h^{\diamond n} - \boldsymbol{u}_h^n\|_{X(\Omega)} + \left\|\frac{(\boldsymbol{u}_h^{\diamond n} - \boldsymbol{u}_h^n) - (\boldsymbol{u}_h^{\diamond n-1} - \boldsymbol{u}_h^{n-1})}{\tau_n}\right\|_{X(\Omega)} \\
&\quad + \sup_{V \in X_0(\Omega)\times L^2(\Omega)} \frac{\langle \mathcal{R}_P, \boldsymbol{V} - \boldsymbol{V}_h\rangle + \langle \mathcal{R}_F, \boldsymbol{V} - \boldsymbol{V}_h\rangle + \langle \mathcal{R}_\Gamma, \boldsymbol{V} - \boldsymbol{V}_h\rangle + \langle \mathcal{F}, \boldsymbol{V} - \boldsymbol{V}_h\rangle}{\|V\|_{X(\Omega)\times L^2(\Omega)}}.
\end{aligned}$$

Then, (61) gives

$$\begin{aligned}
&\|p^n - p_h^n\|_{L^2(\Omega)} + \|\boldsymbol{u}^n - \boldsymbol{u}_h^n\|_{X(\Omega)} + \left\|\frac{(\boldsymbol{u}^n - \boldsymbol{u}_h^n) - (\boldsymbol{u}^{n-1} - \boldsymbol{u}_h^{n-1})}{\tau_n}\right\|_{L^2(\Omega)^d} \\
&\lesssim \|p_h^n - p_h^{\diamond n}\|_{L^2(\Omega)} + (1 + \frac{1}{\tau_n}) \|\boldsymbol{u}_h^n - \boldsymbol{u}_h^{\diamond n}\|_{X(\Omega)} + \frac{1}{\tau_n} \|\boldsymbol{u}_h^{n-1} - \boldsymbol{u}_h^{\diamond n-1}\|_{X(\Omega)} \\
&\quad + \sup_{V \in X_0(\Omega)\times L^2(\Omega)} \frac{\langle \mathcal{R}_P, \boldsymbol{V} - \boldsymbol{V}_h\rangle + \langle \mathcal{R}_F, \boldsymbol{v} - \boldsymbol{V}_h\rangle + \langle \mathcal{R}_\Gamma, \boldsymbol{V} - \boldsymbol{V}_h\rangle + \langle \mathcal{F}, \boldsymbol{V} - \boldsymbol{V}_h\rangle}{\|V\|_{X(\Omega)\times L^2(\Omega)}}.
\end{aligned}$$

To bound the first and the last terms on the right side of the above inequality, we use estimates (51), (52), (53), (54) and the expression of the error indicators η_K^{nP}, η_K^{nF} and $\eta_e^{n\Gamma}$ defined respectively in (47), (48) and (49). Then

$$\begin{aligned}
&\|p^n - p_h^n\|_{L^2(\Omega)} + \|\boldsymbol{u}^n - \boldsymbol{u}_h^n\|_{X(\Omega)} + \left\|\frac{(\boldsymbol{u}^n - \boldsymbol{u}_h^n) - (\boldsymbol{u}^{n-1} - \boldsymbol{u}_h^{n-1})}{\tau_n}\right\|_{L^2(\Omega)^d} \\
&\lesssim \Big(\sum_{K\in\mathcal{T}_{nh}^P} (\eta_K^{nP})^2 + \sum_{K\in\mathcal{T}_{nh}^F} (\eta_K^{nF})^2 + \sum_{e\in\mathcal{E}_{nh}^{P,\Gamma}} (\eta_e^{n\Gamma})^2\Big)^{\frac{1}{2}} + \|p_a^n - p_{ah}^n\|_{H_{00}^{\frac{1}{2}}(\Gamma_{aP})} \\
&\quad + \|\boldsymbol{f}^n - \boldsymbol{f}_h^n\|_{L^2(\Omega_P)^d} + \Big(\sum_{K\in\mathcal{T}_{nh}^F} h_K^2 \|\boldsymbol{f}^n - \boldsymbol{f}_h^n\|_{L^2(K)}^2\Big)^{\frac{1}{2}} \\
&\quad + (1 + \frac{1}{\tau_n}) \|\boldsymbol{u}_h^n - \boldsymbol{u}_h^{\diamond n}\|_{X(\Omega)} + \frac{1}{\tau_n} \|\boldsymbol{u}_h^{n-1} - \boldsymbol{u}_h^{\diamond n-1}\|_{X(\Omega)}.
\end{aligned}$$

Multiplying the square of this inéquality by τ_n, summing over n and using the fact that $\tau_{n+1} \lesssim \sigma_\tau \tau_n$ we deduce

$$\begin{aligned}
&\sum_{n=0}^N \tau_n \Big(\|p^n - p_h^n\|_{L^2(\Omega)}^2 + \|\boldsymbol{u}^n - \boldsymbol{u}_h^n\|_{X(\Omega)}^2 + \left\|\frac{(\boldsymbol{u}^n - \boldsymbol{u}_h^n) - (\boldsymbol{u}^{n-1} - \boldsymbol{u}_h^{n-1})}{\tau_n}\right\|_{L^2(\Omega)^d}^2\Big) \\
&\lesssim \sum_{n=0}^N \tau_n \Big(\sum_{K\in\mathcal{T}_{nh}^P} (\eta_K^{nP})^2 + \sum_{K\in\mathcal{T}_{nh}^F} (\eta_K^{nF})^2 + \sum_{e\in\mathcal{E}_{nh}^{P,\Gamma}} (\eta_e^{n\Gamma})^2\Big) + \sum_{n=0}^N \tau_n \|p_a^n - p_{ah}^n\|_{H_{00}^{\frac{1}{2}}(\Gamma_{aP})}^2 \\
&\quad + \sum_{n=0}^N \tau_n \|\boldsymbol{f}^n - \boldsymbol{f}_h^n\|_{L^2(\Omega_P)^d}^2 + \sum_{n=0}^N \tau_n \Big(\sum_{K\in\mathcal{T}_{nh}^F} h_K^2 \|\boldsymbol{f}^n - \boldsymbol{f}_h^n\|_{L^2(K)}^2\Big) \\
&\quad + \sum_{n=0}^N (\tau_n + \frac{\sigma_\tau}{\tau_{n+1}}) \|\boldsymbol{u}_h^n - \boldsymbol{u}_h^{\diamond n}\|_{X(\Omega)}^2.
\end{aligned} \tag{62}$$

Then the desired estimate follows from (50) and the expression of the indicator $\eta_e^{n\Gamma}$ defined in (49). □

4.3. The efficiency of the indicators

We now establish an upper bound for each indicator η_K^{nP}, η_K^{nF} and $\eta_e^{n\Gamma}$. For this we write the residual equation (55) in a simpler form: For a smooth enough pair $\boldsymbol{V} = (\boldsymbol{v}, q)$,

$$a(\boldsymbol{u}^n - \boldsymbol{u}_h^n, \boldsymbol{v}) + b(\boldsymbol{v}, p^n - p_h^n) + b(\boldsymbol{u}^n - \boldsymbol{u}_h^n, q) + \Big(\frac{(\boldsymbol{u}^n - \boldsymbol{u}_h^n) - (\boldsymbol{u}^{n-1} - \boldsymbol{u}_h^{n-1})}{\tau_n}, \boldsymbol{v}\Big)$$
$$= \mathcal{L}^n(\boldsymbol{v}) - \Big(\frac{(\boldsymbol{u}_h^n - \boldsymbol{u}_h^{n-1})}{\tau_n}, \boldsymbol{v}\Big) - a(\boldsymbol{u}_h^n, \boldsymbol{v}) - b(\boldsymbol{v}, p_h^n) - b(\boldsymbol{u}_h^n, q).$$

Thus, we derive by integration by parts the following residual equation: For a smooth enough pair $\boldsymbol{V} = (\boldsymbol{v}, q)$,

$$a(\boldsymbol{u}^n - \boldsymbol{u}_h^n, \boldsymbol{v}) + b(\boldsymbol{v}, p^n - p_h^n) + b(\boldsymbol{u}^n - \boldsymbol{u}_h^n, q) + \Big(\frac{(\boldsymbol{u}^n - \boldsymbol{u}_h^n) - (\boldsymbol{u}^{n-1} - \boldsymbol{u}_h^{n-1})}{\tau_n}, \boldsymbol{v}\Big)$$
$$= \langle \mathcal{R}_P^*, \boldsymbol{V}\rangle + \langle \mathcal{R}_F, \boldsymbol{V}\rangle + \langle \mathcal{R}_\Gamma^*, \boldsymbol{V}\rangle + \langle \mathcal{F}, \boldsymbol{V}\rangle, \tag{63}$$

where

$$\langle \mathcal{R}_P^*, \boldsymbol{V}\rangle = \sum_{K\in\mathcal{T}_{nh}^P} \Big(\int_K (\boldsymbol{f}_h^n - \frac{\boldsymbol{u}_h^n - \boldsymbol{u}_h^{n-1}}{\tau_n} - \alpha \boldsymbol{u}_h^n)(\boldsymbol{x}) \cdot \boldsymbol{v}(\boldsymbol{x})\, d\boldsymbol{x}$$
$$+ \frac{1}{2} \sum_{e\in\mathcal{E}_K} \int_e \boldsymbol{v}(\tau) \cdot \boldsymbol{n}[p_h^n]_e(\tau)\, d\tau \Big), \tag{64}$$

$$\langle \mathcal{R}_\Gamma^*, \boldsymbol{V}\rangle = \sum_{e\in\mathcal{E}_K^{P,\Gamma}} \int_e \boldsymbol{v}(\tau) \cdot \big((p_h^n \boldsymbol{n})|_{\Omega_P} + (\nu \partial_n \boldsymbol{u}_h^n - p_h^n \boldsymbol{n})|_{\Omega_F}\big)(\tau) d\tau. \tag{65}$$

Due to the choice of the discretization, the next estimate is not optimal: Indeed, Darcy equations are not dimensionless and the variational formulation that we use in order to couple them with the Stokes problem is not appropriate for handling this difficulty (we refer to [43, Chap. XIII], for a more detailed comparison between the different variational formulations); the same lack of optimality appears in [44] for the Darcy equations only and in [6, Prop. 5.4], for another type of coupling Darcy and Stokes problems.

Proposition 6. *The following estimate holds for each error indicator η_K^{nP} defined in (47), $K \in \mathcal{T}_{nh}^P$,*

$$\eta_K^{nP} \lesssim \|\boldsymbol{u}^n - \boldsymbol{u}_h^n\|_{H(\mathrm{div},\omega_K)} + \Big\|\frac{(\boldsymbol{u}^n - \boldsymbol{u}_h^n) - (\boldsymbol{u}^{n-1} - \boldsymbol{u}_h^{n-1})}{\tau_n}\Big\|_{L^2(\omega_K)^d}$$
$$+ h_K^{-1} \|p^n - p_h^n\|_{L^2(\omega_K)} + \|\boldsymbol{f}^n - \boldsymbol{f}_h^n\|_{L^2(\omega_K)^d} + h_K^{-\frac{1}{2}} \|p_a^n - p_{ah}^n\|_{L^2(K\cap\Gamma_{aP})}, \tag{66}$$

where ω_K denotes the union of the elements of $\mathcal{T}_{nh}^P$ that share at least an edge ($d = 2$) or face ($d = 3$) with K.

Proof. For any domain Δ contained in Ω_P, let $R(\Delta)$ denote the right hand-side of (66). We now prove a bound successively for each of the three terms in η_K^{nP}.
(1) Set

$$\boldsymbol{v}_K = \begin{cases} (\boldsymbol{f}_h^n - \dfrac{\boldsymbol{u}_h^n - \boldsymbol{u}_h^{n-1}}{\tau_n} - \alpha \boldsymbol{u}_h^n)\psi_K & \text{on } K, \\ 0 & \text{on } \Omega \setminus K, \end{cases}$$

where ψ_K denotes the bubble function on K, equal to the product of the barycentric coordinates associated with the vertices of K. Inserting $\boldsymbol{v} = \boldsymbol{v}_K$ and $q = 0$ in Eq. (63), we obtain

$$\Big\|(\boldsymbol{f}_h^n - \frac{\boldsymbol{u}_h^n - \boldsymbol{u}_h^{n-1}}{\tau_n} - \alpha \boldsymbol{u}_h^n)\psi_K^{\frac{1}{2}}\Big\|_{L^2(K)^d}^2 \lesssim \|\boldsymbol{u}^n - \boldsymbol{u}_h^n\|_{H(\mathrm{div},K)} \|\boldsymbol{v}_K\|_{L^2(K)^d}$$
$$+ \|p^n - p_h^n\|_{L^2(K)} \|\mathrm{div}\boldsymbol{v}_K\|_{L^2(K)} + \Big\|\frac{(\boldsymbol{u}^n - \boldsymbol{u}_h^n) - (\boldsymbol{u}^{n-1} - \boldsymbol{u}_h^{n-1})}{\tau_n}\Big\|_{L^2(K)^d} \|\boldsymbol{v}_K\|_{L^2(K)^d}$$
$$+ \|\boldsymbol{f}^n - \boldsymbol{f}_h^n\|_{L^2(K)^d} \|\boldsymbol{v}_K\|_{L^2(K)^d} + \|p_a^n - p_{ah}^n\|_{L^2(K\cap\Gamma_{aP})} \|\boldsymbol{v}_K \cdot \boldsymbol{n}\|_{L^2(K\cap\Gamma_{aP})}.$$

Finally, we observe that ψ_K take its values in $[0, 1]$ and we use the following inverse inequalities

$$\|\boldsymbol{v}_K\|_{L^2(K)^d} \lesssim \Big\|\boldsymbol{v}_K \psi_K^{\frac{1}{2}}\Big\|_{L^2(K)^d} \quad \text{and} \quad \|\mathrm{div}\boldsymbol{v}_K\|_{L^2(K)} \lesssim h_K^{-1} \|\boldsymbol{v}_K\|_{L^2(K)^d}.$$

This leads to

$$\left\| \boldsymbol{f}_h^n - \frac{\boldsymbol{u}_h^n - \boldsymbol{u}_h^{n-1}}{\tau_n} - \alpha \boldsymbol{u}_h^n \right\|_{L^2(K)^d} \lesssim R(K). \tag{67}$$

(2) For any $e \in \mathcal{E}_K$, let K' denotes the other element of $\mathcal{T}_{nh}^P$ containing e. Let also $\mathcal{R}_e$ denotes the lifting operator from polynomials on e into polynomials on K, which is built by affine transformation from a fixed lifting operator on the reference element. We now define $\boldsymbol{v}_e$ by

$$\boldsymbol{v}_e = \begin{cases} \mathcal{R}_e([p_h^n]_e)\psi_e & \text{on } K \cup K', \\ 0 & \text{on } \Omega \setminus (K \cup K'), \end{cases}$$

where ψ_e denotes the bubble function on e. By inserting $\boldsymbol{v} = \boldsymbol{v}_e$ and $q = 0$ in Eq. (63), lead to the estimate

$$h_e^{-\frac{1}{2}} \left\| [p_h^n]_e \right\|_{L^2(e)} \lesssim R(K \cup K'). \tag{68}$$

(3) Finally, for any $e \in \mathcal{E}_K^{aP}$, we insert $\boldsymbol{v} = \boldsymbol{v}_e$ and $q = 0$ in Eq. (63), with

$$\boldsymbol{v}_e = \begin{cases} \mathcal{R}_e(p_h^n - p_{ah}^n)\psi_e & \text{on } K, \\ 0 & \text{on } \Omega \setminus K. \end{cases}$$

This leads to

$$h_e^{-\frac{1}{2}} \left\| p_{ah}^n - p_h^n \right\|_{L^2(e)} \lesssim R(K). \tag{69}$$

Combining estimate (67), (68) and (69) leads to the desired result. □

Bounding the η_K^{nF} relies again on the residual equation (63). The arguments are exactly the same as in [45, Prop. 6], for instance, up to the multiplication by $h_K^{-\gamma_K}$ and $h_e^{-\gamma_e}$. So we skip the proof.

Proposition 7. *The following estimate holds for each error indicator η_K^{nF} defined in (48), $K \in \mathcal{T}_{nh}^F$,*

$$\eta_K^{nF} \lesssim h_K^{-\gamma_K} \Big(\left\| \boldsymbol{u}^n - \boldsymbol{u}_h^n \right\|_{H^1(\omega_K)^d} + \left\| \frac{(\boldsymbol{u}^n - \boldsymbol{u}_h^n) - (\boldsymbol{u}^{n-1} - \boldsymbol{u}_h^{n-1})}{\tau_n} \right\|_{L^2(\omega_K)^d}$$
$$+ \left\| p^n - p_h^n \right\|_{L^2(\omega_K)} + h_K \left\| \boldsymbol{f}^n - \boldsymbol{f}_h^n \right\|_{L^2(\omega_K)^d} \Big),$$

where ω_K denotes the union of the elements of $\mathcal{T}_{nh}^F$ that share at least an edge ($d = 2$) or face ($d = 3$) with K.

Due to the lack of homogeneity when coupling Darcy and Stokes equations, the next estimate is not optimal.

Proposition 8. *The following estimate holds for each error indicator $\eta_e^{n\Gamma}$ defined in (49), $e \in \mathcal{E}_{nh}^{P,\Gamma}$,*

$$\eta_e^{n\Gamma} \lesssim h_e^{-1} \left\| \boldsymbol{u}^n - \boldsymbol{u}_h^n \right\|_{X(\omega_e)} + h_e^{-\frac{1}{2}} \left\| p^n - p_h^n \right\|_{L^2(\omega_e)} + h_e^{\frac{1}{2}} \left\| \boldsymbol{f}^n - \boldsymbol{f}_h^n \right\|_{L^2(\omega_e)^d}$$
$$+ h_e^{-\frac{1}{2}} \left\| \frac{(\boldsymbol{u}^n - \boldsymbol{u}_h^n) - (\boldsymbol{u}^{n-1} - \boldsymbol{u}_h^{n-1})}{\tau_n} \right\|_{L^2(\omega_e)^d},$$

where ω_e denotes the union of the element of $\mathcal{T}_{nh}^P$ and the element of $\mathcal{T}_{nh}^F$ that share e.

Proof. Each $e \in \mathcal{E}_{nh}^{P,\Gamma}$ is the edge or face of an element $K \in \mathcal{T}_{nh}^P$ and is contained in the edge or face of an element $K' \in \mathcal{T}_{nh}^F$. We denote by $\tilde{K}'$ the element contained in K' that is constructed from K' by homothety and translation and such that e is an edge or face of $\tilde{K}'$. We now prove a bound successively for each of the two terms in $\eta_e^{n\Gamma}$.
(1) We insert $\boldsymbol{v} = \boldsymbol{v}_e$ and $q = 0$ in Eq. (63), with

$$\boldsymbol{v}_e = \begin{cases} \mathcal{R}_e((p_h^n \boldsymbol{n})|_{\Omega_P} + (\nu \partial_n \boldsymbol{u}_h^n - p_h^n \boldsymbol{n})|_{\Omega_F})\psi_e & \text{on } K \cup \tilde{K}', \\ 0 & \text{on } \Omega \setminus (K \cup \tilde{K}'). \end{cases}$$

This leads

$$\begin{aligned}
&\left\| \left((p_h^n \boldsymbol{n})|_{\Omega_P} + (\nu \partial_n \boldsymbol{u}_h^n - p_h^n \boldsymbol{n})|_{\Omega_F}\right) \psi_e^{\frac{1}{2}} \right\|_{L^2(e)^d}^2 \lesssim \left\| \boldsymbol{u}^n - \boldsymbol{u}_h^n \right\|_{L^2(K)^d} \|\boldsymbol{v}_e\|_{L^2(K)^d} \\
&+ \left\| \boldsymbol{u}^n - \boldsymbol{u}_h^n \right\|_{H^1(\tilde{K}')^d} \|\boldsymbol{v}_e\|_{H^1(\tilde{K}')^d} \\
&+ \left\| p^n - p_h^n \right\|_{L^2(K)} \|\boldsymbol{v}_e\|_{H^1(K)^d} + \left\| p^n - p_h^n \right\|_{L^2(\tilde{K}')} \|\boldsymbol{v}_e\|_{H^1(\tilde{K}')^d} \\
&+ \left\| \frac{(\boldsymbol{u}^n - \boldsymbol{u}_h^n) - (\boldsymbol{u}^{n-1} - \boldsymbol{u}_h^{n-1})}{\tau_n} \right\|_{L^2(K)^d} \|\boldsymbol{v}_e\|_{L^2(K)^d} \\
&+ \left\| \frac{(\boldsymbol{u}^n - \boldsymbol{u}_h^n) - (\boldsymbol{u}^{n-1} - \boldsymbol{u}_h^{n-1})}{\tau_n} \right\|_{L^2(\tilde{K}')^d} \|\boldsymbol{v}_e\|_{L^2(\tilde{K}')^d} \\
&+ \left\| \boldsymbol{f}_h^n - \frac{\boldsymbol{u}_h^n - \boldsymbol{u}_h^{n-1}}{\tau_n} - \alpha \boldsymbol{u}_h^n \right\|_{L^2(K)^d} \|\boldsymbol{v}_e\|_{L^2(K)^d} \\
&+ \left\| \boldsymbol{f}_h^n - \frac{\boldsymbol{u}_h^n - \boldsymbol{u}_h^{n-1}}{\tau_n} + \nu \Delta \boldsymbol{u}_h^n \right\|_{L^2(\tilde{K}')^d} \|\boldsymbol{v}_e\|_{L^2(\tilde{K}')^d} \\
&+ \left\| \boldsymbol{f}^n - \boldsymbol{f}_h^n \right\|_{L^2(K)^d} \|\boldsymbol{v}_e\|_{L^2(K)^d} + \left\| \boldsymbol{f}^n - \boldsymbol{f}_h^n \right\|_{L^2(\tilde{K}')^d} \|\boldsymbol{v}_e\|_{L^2(\tilde{K}')^d}.
\end{aligned}$$

Then, by using several inverse inequalities see [46, Sect. 3.1], we obtain

$$\begin{aligned}
&\left\| (p_h^n \boldsymbol{n})|_{\Omega_P} + (\nu \partial_n \boldsymbol{u}_h^n - p_h^n \boldsymbol{n})|_{\Omega_F} \right\|_{L^2(e)^d} \lesssim h_e^{-\frac{1}{2}} \Big(\left\| \boldsymbol{u}^n - \boldsymbol{u}_h^n \right\|_{X(\omega_e)} \\
&+ \left\| \frac{(\boldsymbol{u}^n - \boldsymbol{u}_h^n) - (\boldsymbol{u}^{n-1} - \boldsymbol{u}_h^{n-1})}{\tau_n} \right\|_{L^2(\omega_e)^d} + \left\| p^n - p_h^n \right\|_{L^2(\omega_e)} + h_K \left\| \boldsymbol{f}^n - \boldsymbol{f}_h^n \right\|_{L^2(\omega_e)^d} \Big).
\end{aligned} \tag{70}$$

(2) Let q be a function in $H^1(K \cup K')$ such that $q = 0$ on $\partial(K \cup K')$. By integration by parts, we obtain

$$\int_e [\boldsymbol{u}_h^n \cdot \boldsymbol{n}]_e(\tau) q(\tau) d\tau = \int_{K \cup \tilde{K}'} \big(\mathrm{div}(\boldsymbol{u}^n - \boldsymbol{u}_h^n)(\boldsymbol{x}) q(\boldsymbol{x}) + (\boldsymbol{u}^n - \boldsymbol{u}_h^n)(\boldsymbol{x}) (\mathbf{grad} q)(\boldsymbol{x}) \big) d\boldsymbol{x}.$$

When we take

$$q = \begin{cases} \mathcal{R}_e([\boldsymbol{u}_h^n \cdot \boldsymbol{n}]_e) \psi_e & \text{on } K \cup \tilde{K}', \\ 0 & \text{on } \Omega \setminus (K \cup \tilde{K}') \end{cases}$$

and using inverse inequalities see [46, Sect. 3.1] we obtain

$$h_e^{-\frac{1}{2}} \left\| [\boldsymbol{u}_h^n \cdot \boldsymbol{n}]_e \right\|_{L^2(e)} \lesssim \left\| \boldsymbol{u}^n - \boldsymbol{u}_h^n \right\|_{X(\omega_e)} + h_e^{-1} \left\| \boldsymbol{u}^n - \boldsymbol{u}_h^n \right\|_{L^2(\omega_e)^d}. \tag{71}$$

Combining estimates (70) and (71) leads to the desired result. □

In Propositions 6–8, the estimates are local in space and time, so that it can be thought that the indicators η_K^{nP}, η_K^{nF} and $\eta_e^{n\Gamma}$ provide a good tool for adapting the mesh.

5. Adaptivity strategy

As standard, the adaptivity strategy that we use combines three steps, an initialization step, an adaptation step in time and an adaptation step in space. We fix a positive tolerance η^* and present it in dimension $d = 2$ for simplicity.

Step 1: Initialization

We fix a triangulation $\mathcal{T}_{0h}^P$ of Ω_P and a triangulation $\mathcal{T}_{0h}^F$ of Ω_F which satisfy Assumptions 2 and 4 and such that the sum of the errors on the five data which appear in Theorem 3, namely

$$\begin{aligned}
&\sum_{n=0}^{N} \tau_n \left\| p_a^n - p_{ah}^n \right\|_{H_{00}^{\frac{1}{2}}(\Gamma_{aP})}^2 \\
&+ \sum_{n=0}^{N} \tau_n \left\| \boldsymbol{f}^n - \boldsymbol{f}_h^n \right\|_{L^2(\Omega_P)^d}^2 + \sum_{n=0}^{N} \tau_n \Big(\sum_{K \in \mathcal{T}_{nh}^F} h_K^2 \left\| \boldsymbol{f}^n - \boldsymbol{f}_h^n \right\|_{L^2(K)}^2 \Big),
\end{aligned}$$

is smaller than η^*. This last condition is possible for smooth data thanks to the approximation properties of the finite element spaces involved in the discretization, and we have no applications for non smooth data.

Step 2: Time adaptivity

Assuming that the time step τ_n, the triangulations $\mathcal{T}^P_{n-1,h}$ and $\mathcal{T}^F_{n-1,h}$ and the discrete solution $(\boldsymbol{u}_h^{n-1}, p_{*h}^{n-1})$ are known, we first choose $\mathcal{T}^P_{nh}$ and $\mathcal{T}^F_{nh}$ equal to $\mathcal{T}^P_{n-1,h}$ and $\mathcal{T}^F_{n-1,h}$, respectively. We compute a first solution $(\boldsymbol{u}_h^n, p_{*h}^n)$ of problem (36) and the corresponding error indicator η_n defined in (38). Next,

• if η_n is smaller than η^*, we proceed to the spatial adaptivity step;
• if not, we divide τ_n by two (or by a constant times η_n/η^*) and perform a new computation.

Of course, this step can be iterated a number of times. This leads to the final value of τ_n.

Step 3: Spatial adaptivity

Assuming that the time step τ_n is known and that the triangulations $\mathcal{T}^P_{nh}$ and $\mathcal{T}^F_{nh}$ are known, we compute the discrete solution of problem (29)–(30)–(31) corresponding to these triangulations, and the error indicators η_K^{nP}, η_K^{nF} and $\eta_e^{n\Gamma}$ defined in (47), (48) and (49).

We denote by $\bar\eta^{nP}$, $\bar\eta^{nF}$ and $\bar\eta^{n\Gamma}$ the mean values of the η_K^{nP}, η_K^{nF} and $\eta_e^{n\Gamma}$, respectively.

Next, we perform adaptivity in three substeps, of course taking into account Assumption 2 in all of them:

• All $e \in \mathcal{E}^{P,\Gamma}_{nh}$ (with obvious notation) such that $\eta_e^{n\Gamma}$ is larger than $\max\{\eta^*, \bar\eta^{n\Gamma}\}$ are divided into N equal segments, where N is proportional to the ratio $\eta_e^{n\Gamma}/\max\{\eta^*, \bar\eta^{n\Gamma}\}$. This gives rise to a new set $e \in \tilde{\mathcal{E}}^{P,\Gamma}_{n+1,h}$.

• The triangulation $\mathcal{T}^F_{nh}$ is refined and coarsened according to the next criterion: The diameter of a new element contained in K or containing K is proportional to h_K times the ratio $\bar\eta^{nF}/\eta_K^{nF}$. This gives rise to the new triangulation $\mathcal{T}^F_{n+1,h}$.

• First, the elements of $\tilde{\mathcal{E}}^{P,\Gamma}_{n+1,h}$ are divided where needed in order that Assumption 4 holds.

Second, a new triangulation on Ω_P is constructed such that these new edges are edges of the elements of the new triangulation.

Next, adaptivity is performed exactly as in the previous substep, now depending on the ratios $\bar\eta^{nP}/\eta_K^{nP}$. This gives rise to the new triangulation $\mathcal{T}^P_{n+1,h}$.

Of course, the adaptation step is iterated either a finite number of times or until the Hilbertian sum of all error indicators, namely

$$\sum_{n=0}^{N}\tau_n\Big(\sum_{K\in\mathcal{T}^P_{nh}}(\eta_K^{nP})^2+\sum_{K\in\mathcal{T}^F_{nh}}(\eta_K^{nF})^2\Big)+\sum_{n=0}^{N}(\tau_n+\frac{\sigma_\tau}{\tau_{n+1}})\Big(\sum_{e\in\mathcal{E}^{P,\Gamma}_{nh}}(\eta_e^{n\Gamma})^2\Big),$$

become smaller than η^*.

References

[1] J. Bear, Hydraulics of Groundwater, McGraw-Hill, New York, 1979.
[2] M. Discacciati, Domain Decomposition Methods for the Coupling of Surface and Groundwater Flows (Ph.D. dissertation), École Polytechnique Fédérale de Lausanne, 2004.
[3] M. Discacciati, E. Miglio, A. Quarteroni, Mathematical and numerical models for coupling surface and groundwater flows, Appl. Numer. Math. 43 (2002) 57–74.
[4] W.L. Wood, Introduction To Numerical Methods for Water Resources, Oxford University Press, 1993.
[5] C. Bernardi, T. Chacón. Rebollo, F. Hecht, Z. Mghazli, Mortar finite element discretization of a model coupling Darcy and Stokes equations, ESAIM: M2AN 42 (2008) 375–410.
[6] C. Bernardi, F. Hecht, O. Pironneau, Coupling darcy and stokes equations for porous media with craks, ESAIM: M2AN 39 (2005) 7–35.
[7] E. Burman, P. Hansbo, A unified stabilized method for Stokes' and Darcy's equations, J. Comput. Appl. Math. 198 (2007) 35–51.
[8] G.N. Gatica, S. Meddahi, R. Oyarzúa, A conforming mixed finite element method for the coupling of fluid flow with porous media flow, IMA J. Numer. Anal. 29 (2009) 86–108.
[9] G.N. Gatica, R. Oyarzúa, F.-J. Sayas, Analysis of fully-mixed finite element methods for the Stokes-Darcy coupled problem, Math. Comp. 80 (276) (2011) 1911–1948.
[10] G. Kanschat, B. Rivière, A strongly conservative finite element method for the coupling of Stokes and Darcy flow, J. Comput. Phys. 229 (17) (2010) 5933–5943.
[11] W.J. Layton, F. Schieweck, I. Yotov, Coupling fluid flow with porous media flow, SIAM J. Numer. Anal. 40 (2003) 2195–2218.
[12] B. Rivière, Analysis of a discontinuous finite element method for the coupled Stokes and Darcy problems, J. Sci. Comput. 22 (2005) 479–500.
[13] B. Rivière, I. Yotov, Locally conservative coupling of Stokes and Darcy flows, SIAM J. Numer. Anal. 42 (5) (2005) 1959–1977.
[14] C. Wenbin, Y. Wang, A posteriori error estimate for the H(div) conforming mixed finite element for the coupled Darcy-Stokes system, J. Comput. Appl. Math. 255 (2014) 502–516.
[15] G.S. Beavers, D. Joseph, Boundary conditions at a naturally permeable wall, J. Fluid Mech. 30 (1967) 197–207.
[16] D.-G. Calugaru, Modélisation et Simulation Numérique du Transport de Radon dans un Milieu Poreux Fissuré ou Fracturé. Problème Direct et Problèmes Inverses Comme Oulils D'aide à la Prédiction Sismique (Ph.D. thesis), Université de Franche-Comté, Besançon, France, 2002.
[17] M. Kubacki, M. Moraiti, Analysis of a second-order, unconditionally stable, partitioned method for the evolutionary Stokes-Darcy model, Int. J. Numer. Anal. Model. 12 (2015) 704–730.
[18] W. Layton, H. Tran, C. Trenchea, Analysis of long time stability and errors of two partitioned methods for uncoupling evolutionary groundwater-surface water flows, SIAM J. Numer. Anal. 51 (2015) 248–272.
[19] W. Layton, H. Tran, X. Xiong, Long time stability of four methods for splitting the evolutionary Stokes-Darcy problem into Stokes and Darcy subproblems, J. Comput. Appl. Math. 236 (2012) 3198–3217.

[20] C. Bernardi, Y. Maday, A.T. Patera, A new nonconforming approch to domain decomposition: the motor element method, in: H. Brezis, J.-L. Lions (Eds.), Collège de France Seminar XI, Pitman, 1994, pp. 13–51.
[21] C. Bernardi, Y. Maday, F. Rapetti, Basics and some applications of the motar element method, GAMM-Ges. Angew. Math. Mech. 28 (2005) 97–123.
[22] M. Fortin, Old and new elements for incompressible flows, Internat. J. Numer. Methods Fluids 1 (1981) 347–364.
[23] C. Bernardi, G. Raugel, Analysis of some finite elements for the Stokes problem, Math. Comp. 44 (1985) 71–79.
[24] P.-A. Raviart, J.-M. Thomas, A mixed finite element method for second order elliptic problems, in: Mathematical Aspects of Finite Element Methods, in: Lect. Notes Math., vol. 606, Springer, 1977, pp. 292–315.
[25] C. Bernardi, A. Younes. Orfi, A Priori error analysis of the fully discretized time-dependent coupled Darcy and Stokes equations, J. Spanish Soc. Appl. Math. SeMA 73 (2) (2016) 97–119.
[26] C. Bernardi, B. Métivet, Indicateurs d'erreur pour l'équation de la chaleur, Rev. Eur. Élém. Finis. 9 (2000) 425–438.
[27] M. Bieterman, Babuška, The finite element method for parabolic equations. I. A posteriori error estimation, Numer. Math. 40 (1982) 339–371.
[28] M. Bieterman, Babuška, The finite element method for parabolic equations. II. A posteriori error estimation and adaptive approach, Numer. Math. 40 (1982) 373–406.
[29] K. Eriksson, C. Johnson, Adaptive finite element methods for parabolic problems. I. A linear model problem, SIAM J. Numer. Anal. 28 (1991) 43–77.
[30] K. Eriksson, C. Johnson, Adaptive finite element methods for parabolic problems. IV. Nonlinear problems, SIAM J. Numer. Anal. 32 (1995) 1729–1749.
[31] R. Verfürth, A posteriori error estimates techniques for non-linear elliptic and parabolic pdes, Rev. Eur. Élém. Finis. 9 (2000) 377–402.
[32] A. Bergam, C. Bernardi, Z. Mghazli, A posteriori analysis of the finite element discretization of some parabolic equations, Math. Comp. 74 (2005) 1117–1138.
[33] Y. Achdou, C. Bernardi, Un schéma de volumes ou éléments finis adaptatif pour les équations de Darcy à perméabilité variable, C. R. Acad. Sci., Paris Sér. I 333 (2001) 693–698.
[34] C. Bernardi, F. Hecht, Z. Mghazli, Mortar finite element discretization for the flow in a non homogeneous porous medium, Comput. Methods Appl. Mech. Engrg. 196 (2007) 1554–1573.
[35] R. Lewandowski, Analyse mathémathique et océanographie, in: Collection Recherches En Mathématiques Appliquées, Masson, 1997.
[36] V. Girault, P.-A. Raviart, Finite Element Methods for Navier Stokes Equations, Theory and Algorithms, in: Springer Series in Computational Mathematics, vol. 5, Springer-Verlag, 1986.
[37] J.-L. Lions, E. Magenes, Problèmes Aux Limites Non Homogènes Et Applications, Vol. 1, Dunod, 1968.
[38] J.-C. Nédélec, Mixed finite elements in $\mathbb{R}^3$, Numer. Math. 35 (1980) 315–341.
[39] F. Ben Belgacem, The Mortar finite element method with Lagrangian multiplier, Numer. Math. 84 (1999) 173–197.
[40] C. Johnson, Y.-Y. Nie, V. Thomée, An a posteriori error estimate and adaptive timestep control for a backward Euler discretization of a parabolic problem, SIAM J. Number. Anal. 27 (1990) 277–291.
[41] C. Carstensen, J. Hu, A unifying theory of a posteriori error control for nonconforming finite element methods, Numer. Math. 107 (2007) 473–502.
[42] Y. Achdou, C. Bernardi, F. Coquel, A priori and a posteriori analysis of finite volume discretizations of Darcy's equations, Numer. Math. 96 (2003) 17–42.
[43] C. Bernardi, Y. Maday, F. Rapetti, Discrétisations Variationnelles de Problèmes Aux Limites Elliptiques, in: Collection Mathématiques et Applications, vol. 45, Springer-Verlag, 2004.
[44] D. Braess, R. Verfürth, A posteriori error estimators for the Raviart–Thomas element, SIAM J. Numer. Anal. 33 (1996) 2431–2444.
[45] C. Bernardi, B. Métivet, R. Verfürth, in: P.-L. George (Ed.), Analyse numérique d'indicateurs d'erreur, dans Maillage et adaptation, Hermès, 2001, pp. 251–278 (Chapter 8), édité par. http://www.ann.jussieu.fr/hecht/ftp/Ecole-Cirm-EFEF5/Bernardi-Cours.pdf.
[46] R. Verfürth, A Review of a Posteriori Error Estimation and Adaptive Mesh-Refinement Techniques, Wiley Teubner, 1996.